AD-A117 702 BATTELLE COLUMBUS LABS OH F/G 11/8
THERMAL EFFECTS IN ROLLING/SLIDING CONTACT.(U)
JUL 82 T A DOW, R D STOCKWELL, T L MERRIMAN N00014-81-C-0608
UNCLASSIFIED BATT-G-7818-0001 NL

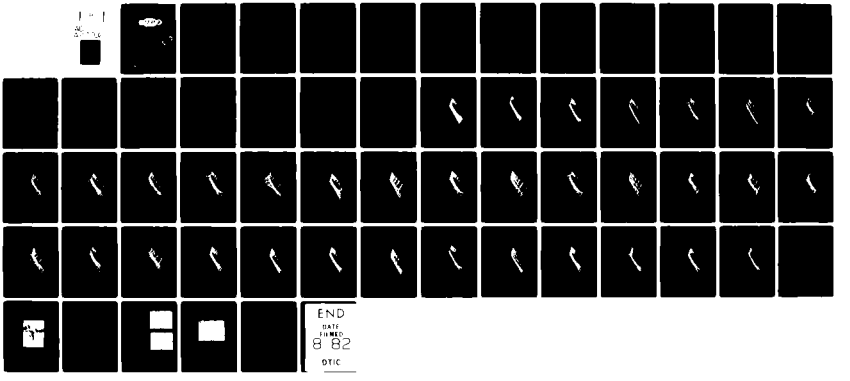

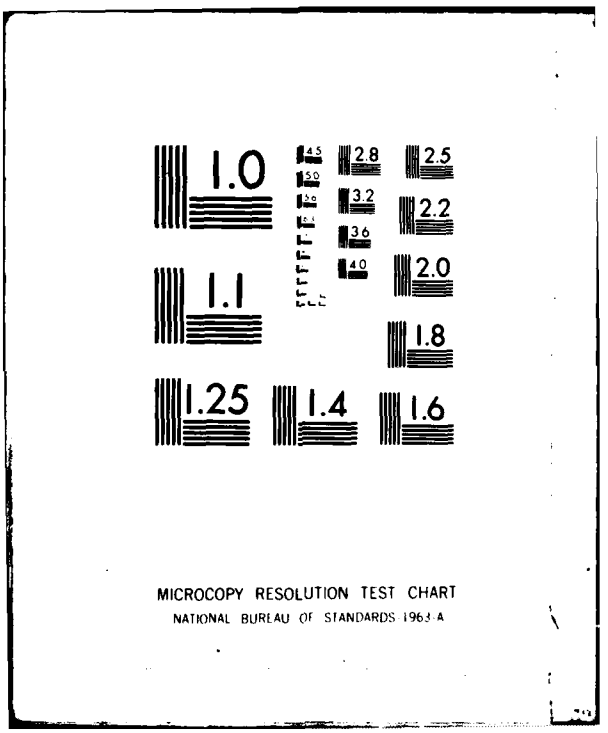
1.0
1.1
1.25
1.4
1.6
1.8
2.0
2.2
2.5
2.8
3.2
3.6
4.0
4.5
5.0
5.6
6.3
7.1
MICROCOPY RESOLUTION TEST CHART
NATIONAL BUREAU OF STANDARDS 1963-A

(12)

REPORT N00014-81-C-0608

THERMAL EFFECTS IN ROLLING/SLIDING CONTACT

T. A. DOW
R. D. STOCKWELL
T. L. MERRIMAN
J. W. KANNEL

BATTELLE
COLUMBUS LABORATORIES
505 KING AVENUE
COLUMBUS
OHIO
43201

31 JULY 1982

FINAL REPORT FOR PERIOD COVERED 1 JUNE 81 - 31 MAY 82

Approved for public release; distribution unlimited.

PREPARED FOR THE

OFFICE OF NAVAL RESEARCH • 800 NORTH QUINCY ST • ARLINGTON • VA • 22217

DCASMA, DAYTON • DEFENSE ELECTRONICS SUPPLY CENTER
• 1502 WILMINGTON PIKE • DAYTON • OH • 45444

SECURITY CLASSIFICATION OF THIS PAGE (When Data Entered)

REPORT DOCUMENTATION PAGE		READ INSTRUCTIONS BEFORE COMPLETING FORM
1. REPORT NUMBER	2. GOVT ACCESSION NO. AD-A117102	3. RECIPIENT'S CATALOG NUMBER
4. TITLE (and Subtitle) Thermal Effects in Rolling/Sliding Contact		5. TYPE OF REPORT & PERIOD COVERED Final Report June 1, 1981 - May 31, 1982
		6. PERFORMING ORG. REPORT NUMBER G7813-0001
7. AUTHOR(s) T. A. Dow, R. D. Stockwell, T. L. Merriman and J. W. Kannel		8. CONTRACT OR GRANT NUMBER(s) N00014-81-C-0608
9. PERFORMING ORGANIZATION NAME AND ADDRESS Battelle Columbus Laboratories 505 King Avenue Columbus, Ohio 43201		10. PROGRAM ELEMENT, PROJECT, TASK AREA & WORK UNIT NUMBERS
11. CONTROLLING OFFICE NAME AND ADDRESS Office of Naval Research 800 North Quincy Street Arlington, Virginia 22217		12. REPORT DATE July 31, 1982
		13. NUMBER OF PAGES 56
14. MONITORING AGENCY NAME & ADDRESS(if different from Controlling Office) DCASMA, Dayton Defense Electronics Supply Center 1502 Wilmington Pike Dayton, Ohio 45444		15. SECURITY CLASS. (of this report) Unclassified
		15a. DECLASSIFICATION/DOWNGRADING SCHEDULE

16. DISTRIBUTION STATEMENT (of this Report)

Approved for public release, distribution unlimited.

17. DISTRIBUTION STATEMENT (of the abstract entered in Block 20, if different from Report)

18. SUPPLEMENTARY NOTES

19. KEY WORDS (Continue on reverse side if necessary and identify by block number)

Elastohydrodynamic lubrication, temperature transducer, pressure transducer, film thickness, rolling contact, slip, 3-dimensional mapping, local traction measurement

20. ABSTRACT (Continue on reverse side if necessary and identify by block number)

This report discusses the results of a series of pressure and temperature distributions measured between a pair of elastohydrodynamically (EHD) lubricated disks. Three lubricants have been studied: a synthetic paraffinic oil (XRM-109F), polyphenyl ether (OS-124), and a traction fluid (Santotrac 50). Pressure and temperature readings throughout the contact are presented as three-dimensional plots. Measurements of the EHD film thickness, and the tractive force between disks under slip conditions are also presented.

Continued

DD FORM 1 JAN 73 1473 EDITION OF 1 NOV 65 IS OBSOLETE

SECURITY CLASSIFICATION OF THIS PAGE (When Data Entered)

(20) A method for one-dimensional mapping of tractive force is introduced. An instrumental part of the method is the data handling capability of a digitizing oscilliscope which captures signals from a traction probe. The oscilliscope's capabilities are greatly expanded by a microprocessor which controls its functions. Preliminary results from this method of local traction measurement are presented.

TABLE OF CONTENTS

	Page
SUMMARY	1
INTRODUCTION	1
MAPPING THE CONTACT PRESSURE AND TEMPERATURE	3
Apparatus	3
Lubricant Properties	4
Experimental Procedure	5
Experimental Results	6
Discussion	9
MAPPING THE LOCAL SHEAR STRESS	10
Approach	10
Apparatus	11
Experimental Procedure and Results	11
Discussion	12
CONCLUSIONS	13
REFERENCES	53

LIST OF TABLES

Table 1. Disk Load and Resulting Contact Geometry	4
Table 2. Lubricant Properties	4
Table 3. Measured Film Thickness and Traction Data	7

LIST OF FIGURES

Figure 1. Surface pressure and temperature distribution for XRM-109F at 59C and 0.0 percent slip	14
Figure 2. Surface pressure and temperature distribution for XRM-109F at 59C and 0.0 percent slip	16

LIST OF FIGURES

(Continued)

		Page
Figure 3.	Surface pressure and temperature distribution for XRM-109F at 59C and 0.0 percent slip	18
Figure 4.	Surface pressure and temperature distribution for XRM-109F at 58C and 5.8 percent slip	20
Figure 5.	Surface pressure and temperature distribution for XRM-109F at 58C and 5.3 percent slip	22
Figure 6.	Surface pressure and temperature distribution for XRM-109F at 63C and 6.2 percent slip	24
Figure 7.	Surface pressure and temperature distribution for OS-124 at 75C and 0.0 percent slip	26
Figure 8.	Surface pressure and temperature distribution for OS-124 at 72C and 0.0 percent slip	28
Figure 9.	Surface pressure and temperature distribution for OS-124 at 72C and 0.0 percent slip	30
Figure 10.	Surface pressure and temperature distribution for OS-124 at 77C and 5.9 percent slip	32
Figure 11.	Surface pressure and temperature distribution for OS-124 at 76C and 4.4 percent slip	34
Figure 12.	Surface pressure and temperature distribution for OS-124 at 81C and 3.5 percent slip	36
Figure 13.	Surface pressure and temperature distribution for Santotrac 50 at 24C and 0.0 percent slip	38
Figure 14.	Surface pressure and temperature distribution for Santotrac 50 at 24C and 0.0 percent slip	40
Figure 15.	Surface pressure and temperature distribution for Santotrac 50 at 24C and 0.0 percent slip	42
Figure 16.	Surface pressure and temperature distribution for Santotrac 50 at 27C and 5.5 percent slip	44
Figure 17.	Surface pressure and temperature distribution for Santotrac 50 at 29C and 2.0 percent slip	46

LIST OF FIGURES

(Continued)

		Page
Figure 18.	Traction transducer entering contact region of rolling disk	48
Figure 19.	Local traction transducer and mated test disk . . .	49
Figure 20.	Cross section of disc showing details of traction measurement paddle	50
Figure 21.	Traction transducer output	51
Figure 22.	Differentiated traction transducer output	52

THERMAL EFFECTS IN ROLLING/SLIDING CONTACTS

by

T. A. Dow, R. D. Stockwell,
T. L. Merriman and J. W. Kannel

SUMMARY

This report discusses the results of a series of pressure and temperature distributions measured between a pair of elastohydrodynamically (EHD) lubricated disks. Three lubricants have been studied: a synthetic paraffinic oil (XRM-109F), polyphenyl ether (OS-124), and a traction fluid (Santotrac 50). Pressure and temperature readings throughout the contact are presented as three-dimensional plots. Measurements of the EHD film thickness, and the tractive force between disks under slip conditions are also presented. Data are presented for one surface speed, three values of disk load, and two values of slip. A method for one-dimensional mapping of tractive force is introduced. An instrumental part of the method is the data handling capability of an digitizing oscilliscope which captures signals from a traction probe. The oscilliscope's capabilities are greatly expanded by a microprocessor which controls its functions. Preliminary results from this method of local traction measurement are presented.

INTRODUCTION

One of most important parameters of a rolling/sliding contact is also one of the least defined, and that is the interface temperature. In a journal bearing, the heat is generated by shear of the fluid between the journal and shaft. Most of the heat generation occurs in the high pressure region where the clearance is at a minimum. The heat generation in this area affects the fluid properties and, thus, the friction throughout the lubricant film.

In an EHD contact, the situation is more complicated. The elastic deflections of the mating parts define the geometry of the contact and the fluid flow through this region defines the heat generation, which in turn influences the properties of the lubricant.

It has only been in recent years that the surface temperature in EHD contacts has been measured. In a program for ONR, Kannel and Dow[1]* have measured temperature distributions (as well as pressure) in EHD contacts using surface transducers. These transducers are vapor-deposited thin metallic films whose resistances are functions of temperature and pressure. The technique allows simultaneous measurements of pressure and temperature on one small region of the disk surface as it moves through the high pressure region. This data has been used in an analysis[2] of the sources and sinks for heat generation in the contact. The analysis was carried out for several oils, assuming a Newtonian fluid model. The results were extremely interesting; however, the heating terms did not exactly balance the dissipation terms.

The past experiments have produced a picture of the temperature and pressure distribution through the center of the contact. In the section entitled, Mapping the Contact Pressure and Temperature, the current experiments extend that view to the whole interface and 3-D plots of the pressure and temperature have been produced. These experiments have also included measurements of the film thickness and traction which existed during the pressure and temperature movements. In this manner, a complete picture of the contact has been developed for the whole contact region.

The second part of this report, Mapping the Local Shear Stress, deals with an innovation in traction measurement. In addition to the conventional method of measuring a traction value which represents an average over the entire contact region, a traction transducer which measures tractive force as a function of position in the contact region has been devised. The basis of this new device is a small paddle which is machined into a cylindrical disk. When the paddle comes into rolling contact with another disk, the traction produces a deflection of the paddle which can be used to determine the tractive forces. Preliminary theory and operation of this device is presented along with some initial experimental results.

---

*References are listed on page 53.

MAPPING THE CONTACT PRESSURE AND TEMPERATURE

Apparatus

The data was generated on a twin-disk machine (described in Reference 1) which consists of a pair of 35.6-mm (nominal diameter) disks, independently driven by 1.25 hp drive motors. The nominal motor speed during the experiments was 5,000 rpm. For operation at this speed, the motor can generate a maximum force to produce slip between the disk of 89 N (20 pounds). This situation was limited to the slip which could be imposed on the traction fluid at the higher values of disk loading.

The upper disk is a crowned, cylindrical disk whereas the lower disk is a pure cylinder. The diameter of the lower disk is 35.7 mm (1.4 inches). The upper disk has a crown radius of 205.7 mm (8.1 inches) and a diameter in the center of 35.458 mm (1.396 inches). This diameter variation means that the disks must be run at a small indicated slip value to be in true rolling contact.

The disk speeds are measured by electronic counters which read the pulses from a 60-tooth pickup on each motor shaft. The value of the slip between the disk surfaces is measured by a ratio meter which gives the ratio of the upper disk speed to the lower disk speed. For the disk diameters given above, the indicated slip for the case of pure rolling would be 1.0068. This value was corroborated during the slip experiments for the traction fluid where if the disks were taken out of contact at this value of slip, little or no change in traction occurred.

The disk load was applied by a deadweight system with a mechanical advantage of 11.4 to 1.0. Table 1 shows the disk load and the dimensions of the contact for each of the load values studied. The equivalent Hertzian stress for each load is also shown in the table and the values range from 0.9 GPa (130.0 ksi) to 1.4 GPa (203.8 ksi). This load range includes severe loading for common machine elements.

TABLE 1. DISK LOAD AND RESULTING CONTACT GEOMETRY

Hanger load, N	Disk load, N	Half-Width of Hertzian Contact, mm	Half-length of Hertzian Contact, mm	Maximum Hertzian Stress, GPa
22	254	1.026	.132	0.89
40	454	1.250	.160	1.07
58	658	1.417	.183	1.22
85	970	1.605	.206	1.39

Lubricant Properties

Three lubricant properties were studied during the experiments reported. Two of these lubricants (XRM-109F and OS-124) were supplied by Mr. R. J. Parker of NASA-Lewis Research Center. Limited property data for these lubricants are shown in Table 2.

TABLE 2. LUBRICANT PROPERTIES

Lubricant		Viscosity, cp		Test temp, °C	Test viscosity, cp
Designation	Description	38°C	100°C		
XRM-109F	Synthetic paraffinic hydrocarbon	360	32	58	130
OS-124	Polyphenyl ether	450	15	77	40
SANTOTRAC 50		39	5	25	53

The lubricant temperature during the experiments was selected to produce sufficiently low viscosity to allow easy pumping of the lubricant but high enough to produce thick hydrodynamic films both to protect the pressure and temperature transducers from damage and to produce EHD rather than boundary lubricated contact.

The test temperature and viscosity of each fluid is also shown in Table 2. The lubricant with the highest viscosity was the synthetic

paraffinic (XRM-109F) at 130 cp and the polyphenyl ether (OS-124) had the lowest viscosity at 40 cp.

Experimental Procedure

The main objective of the experiments was to develop simultaneous pressure and temperature data for different lubricants under EHD operating conditions. As described in an earlier section, the surface pressure and temperature were sensed by surface coatings whose active dimensions were 0.05 mm (0.002 inch) along the length of the contact and 0.10 mm (0.0039 inch) across the width of the contact. For the lowest load, these dimensions are less than 20 percent of the length and 5 percent of the width and at the maximum load they become 12 percent and 3 percent, respectively. These relative dimensions show that the pressure transducer is long compared to the length of the contact and, therefore, some details of the pressure trace (e.g., the "pressure spike" at the outlet edge of the contact) were lost due to the pressure signal being averaged over the width of the transducer.

During the experiments, it was noted that neither the pressure nor the temperature trace was steady, but rather the signals varied slightly for each passage through the conjunction region. Therefore, both the pressure and temperature signals were averaged over 25 revolutions of the disk.

The experimental procedure which was developed involved loading the disks in contact at the specified test conditions (disk load, temperature, and slip). At the start of each test, the lower disk was positioned such that the transducer was near the center of the contact. The pressure and temperature traces were recorded successively (average of 25 revolutions each), then the disk was unloaded, the lower disk moved 0.050 mm (0.0020 inch) to the right (or left), and reloaded. The lower disk was moved in 0.51-mm steps until the pressure and temperature readings went to zero. This disk was then moved back to the center and moved through the other side of the contact. When the entire contact was plotted, the next load was applied and the procedure repeated. For each lubricant, the pressure and temperature traces were plotted for 0.0 percent slip at each load and then for the 5.0 percent slip condition.

While the pressure and temperature data were being generated, the X-ray system was used to measure the minimum separation of the disks and the traction load cell recorded the tractive force between the disks. This data should fully describe the contact conditions for future thermal analysis of the contact.

Experimental Results

The pressure and temperature data generated during the experiments are shown in Figures 1 through 17 and measured data for film thickness and traction are shown in Table 3. The figures are presented in two parts: Part A is the pressure distribution and Part B is the matching temperature distribution.

The pressure and temperature profiles are presented on a coordinate system whose relative proportions are similar to the actual geometry of the contact. The length direction is the direction of rolling and each division represents 3.12×10^{-3} mm (0.123×10^{-3} inch). The width dimension is along the cylinder axis and each division represents 0.51 mm (0.020 inch). The pressure and temperature readings were taken at each width division and each 10th point is connected by a straight line to produce the surfaces shown.

Figure 1A and 1B show the pressure and temperature distribution at a disk loading of 254 Newtons. The peak pressure is 0.89 GPa (130 ksi) and the peak temperature is 13°C. It is clear from the figure that these two peaks do not coincide; the pressure peak occurs at about 400 length units whereas the temperature peak occurs at about 350 units. The relative length of the contact for these figures is 85 units. Therefore, for this pure rolling condition, the peak temperature occurs in the inlet region. This same result was described in the earlier work[1].

Figures 2 and 3 are for 102 and 218 pounds (454 and 970 N) disk loading respectively. For Figure 2, the peak pressure is nearly 1.07 GPa (156 ksi) and the peak temperature is 14°C. The peak pressure in Figure 3 is 1.39 GPa (203 ksi) and the temperature peak is 15°C.

TABLE 3. MEASURED FILM THICKNESS AND TRACTION DATA

Figure	Peak Pressure GPa	Peak Pressure (ksi)	Lubricant	Disk Temp[a], °C	Viscosity, cp	Film Thickness mm x 10^3	Film Thickness in. x 10^6	Slip, percent	Traction N	Traction (lbs)	Peak surface temp, °C
1	0.89	(130)	XRM-109F	55	125	3.3	(133)	0.0	0.0	(0.0)	13
2	1.07	(156)	XRM-109F	65	125	2.5	(98)	0.0	0.0	(0.0)	14
-	1.22	(177)	XRM-109F	60	125	2.3	(93)	0.0	0.0	(0.0)	--
3	1.39	(203)	XRM-109F	64	125	1.8	(73)	0.0	0.0	(0.0)	15
4	0.89	(130)	XRM-109F	58	130	1.8	(71)	5.8	4.0	(<1.0)	15
5	1.07	(156)	XRM-109F	58	130	1.6	(62)	5.3	8.8	(2.0)	18
6	1.39	(203)	XRM-109F	63	110	1.3	(50)	6.2	22.2	(5.0)	28
7	0.89	(130)	OS-124	80	36	1.5	(59)	0.0	0.0	(0.0)	7
8	1.07	(156)	OS-124	76	40	1.4	(54)	0.0	0.0	(0.0)	5
-	1.22	(177)	OS-124	80	40	1.3	(50)	0.0	0.0	(0.0)	--
9	1.39	(203)	OS-124	76	40	1.1	(45)	0.0	0.0	(0.0)	5
10	0.89	(130)	OS-124	77	34	1.8	(69)	5.9	2.2	(0.5)	24
11	1.07	(156)	OS-124	76	35	1.4	(54)	4.4	8.9	(2.0)	27
12	1.22	(177)	OS-124	81	28	1.1	(45)	3.5	22.2	(5.0)	20

TABLE 3. CONTINUED

Figure	Peak Pressure GPa	(ksi)	Lubricant	Disk Temp[a], °C	Viscosity, cp	Film Thickness mm x 10^3	in. x 10^6	Slip, percent	Traction N	(lbs)	Peak surface temp, °C
13	0.89	(130)	SANTOTRAC 50	31	57	2.3	(92)	0.0	0.0	(0.0)	9
14	1.07	(156)	SANTOTRAC 50	32	57	2.0	(79)	0.0	0.0	(0.0)	6
--	1.22	(177)	SANTOTRAC 50	36	57	1.8	(73)	0.0	0.0	(0.0)	--
15	1.39	(203)	SANTOTRAC 50	39	57	1.4	(56)	0.0	0.0	(0.0)	6
16	0.89	(130)	SANTOTRAC 50	27	50	1.9	(74)	5.5	7.8	(1.8)	50
17	1.07	(156)	SANTOTRAC 50	29	43	1.8	(69)	2.0	40.9	(9.2)	30
--	0.89	(130)	SANTOTRAC 50	70	--	.83	(33)	0.0	0.0	(0.0)	--
--	1.07	(156)	SANTOTRAC 50	76	--	.63	(25)	0.0	0.0	(0.0)	--
--	1.22	(177)	SANTOTRAC 50	71	--	.63	(25)	0.0	0.0	(0.0)	--
--	1.39	(203)	SANTOTRAC 50	72	--	.60	(24)	0.0	0.0	(0.0)	--

(a) Some disk temperatures vary slightly from those values listed on figure titles.

For these three pure rolling cases, (Figures 1, 2, and 3), the peak temperature occurs in the inlet zone of the contact. Figures 4 through 6 show the pressure and temperature for 5-6 percent slip. As shown in Table 3, the peak temperature is proportional to the load (and therefore the traction), the peak temperature for the highest load being twice that of the pure rolling condition.

Figures 7 through 9 are for pure rolling conditions using the polyphenyl ether (OS-124). These pure rolling cases show very low surface temperatures, about half the values measured for the synthetic paraffinic lubricant previously discussed. The surface temperatures measured using the OS-124 were essentially independent of the loading.

The slip cases studied for polyphenyl ether are shown in Figures 10 through 12. Table 3 shows the slip is not constant for these three cases due to experimental control; however, the peak temperatures measured during these experiments are above 20°C or more than 4 times the pure rolling values.

The pure rolling experiments with the traction fluid (Santotrac 50) are shown in Figures 13 through 15. These pure rolling cases show peak temperatures in the range measured for the other two oils 6-9°C. However, when slip is developed using this lubricant, the tractive force and the peak temperature rise rapidly. The highest surface temperature rise was measured with this lubricant at the low disk load and 5.5 percent slip; this surface temperature peak was 50°C (figure 16B). At the higher disk loading (Figure 17), the slip was conservatively limited to 2.0 percent, but the temperature rise still exceeded 30°C.

Discussion

The objective of these experiments has been to generate experimental temperature and pressure data for a variety of lubricant chemistries. These data will be used to refine a thermal model of contact process which can be used to estimate the heating and the temperature rise for other lubricants and operating conditions.

The data presented in this report shows marked differences in temperature as a function of the lubricant, both at pure rolling and

rolling/sliding conditions. This data should provide the necessary experimental corroboration for the analytical heat balance, which will be developed in another project.

MAPPING THE LOCAL SHEAR STRESS

Approach

As a lubricant enters into the elastohydrodynamic contact region, its behavior changes markedly from that at ambient conditions. For example, the pressure and temperatures discussed previously cause significant change in lubricant viscosity and, possibly, even in the physical state of the fluid. It is possible, for example, that the fluid enters into a glass transition state[3]. Various researchers[4-8] have attempted to define this state of the fluid by theoretical and indirect experimental measurement.

One goal of these models is to understand the shear stress in the fluid with the objective of predicting fluid traction. If it were possible to measure shear stress at a point and then sweep this point through the contact region, you would have a shear measurement which is only a function of position. The integral of this shear stress over the contact area is the tractive force, F_T.

$$F_T = \int_A T(x)\ dA \quad .$$

Here $T(x)$ is the shear stress as a function of position and A is the contact area.

Figure 18 is a schematic drawing of a method of measuring the shear stress. The diagram shows two disks in rolling contact. The lower disk has slots milled into the surface to form a paddle. The shear stress on the paddle from the contact with the other disk deflects the paddle as a simple beam which is end loaded. The beam is extended axially to provide a surface for a proximity probe to bear on to measure deflection. The paddle and probe are described in detail in the experimental apparatus. The output from the

the probe represents the integral of the shear stress over the entire contact region. The derivative of this signal is a continuous function which shows the tractive force level at each position of the contact zone.

Apparatus

The traction measurement device consist of two 36.118-mm (1.422 inches) center diameter disks, mounted in the same twin disk machine used in the experiments described earlier. These disks are shown in Figures 19 and 20. Both disks are 6.350 mm (0.250 inch) wide. The upper disk has a 139.7-mm (5.5 inches) crown radius.

The lower disk is cylindrical with the following modifications. Three .203 mm (.008 inch) slots have been machined across the face, by the electric discharge method, to form two paddles. These paddles are .508 mm (.020 inch) thick circumferentially, 2.54 mm (0.10 inch) deep radially, and are 6.350 mm (.250 inch) wide at the base. The tip of the paddle has a flap which extends axially. This flap provides a surface for a proximity probe to bear on. These details of the flap are shown in Figure 20. The proximity probe used is a Kaman KD2300-5SU, which is sensitive to motions on the order of 254×10^{-6} mm (10×10^{-6} inch).

The output from the probe is received by a microprocessor-controlled digitizing oscilliscope which stores and manipulates results as described in the experimental procedure.

Experimental Procedure and Results

The two disk were brought into contact and the lower disk driven at approximately 120 rpm. They were then loaded to approximately 1.4 GPa (200 ksi). Approximately 31 Newtons (7 pounds) of traction was applied to the upper disk. The disks were coated with a light film of high viscosity oil.

The deflection of the paddle on the lower disk was picked up by the proximity probe and transferred through a slip ring to the oscilliscope. The oscilliscope digitizes analog signals at a high resolution of 1012 points per pulse (10 cm screen, horizontally). Since the traction signal varied slightly with each pass, the capability of the oscilliscope controller to

acquire an average signal was applied over 10-25 revolutions. The signal was next smoothed. Smoothing of the signal removes system noise which imposes a high frequency ripple on top of the proximity probe's output. Without this smoothing capability, the derivative of the signal is rendered undecipherable by the derivative of the noise component. The resultant acquired, averaged, and smoothed signal is shown in Figure 21(a).

The next step was to perform a differentiating algorithm on the signal, as previously discussed, to arrive at Figure 21(b). The oscilliscope further allows us to section off the inlet and outlet portions of this traction signal and invert the inlet section. This produces the comparison of Figures 22(a) and 22(b) which shows these two traces offset by one vertical division.

Discussion

This effort in shear stress measurement is, of course, very rudimentary and must be considered quite tentative. However, it is interesting to speculate what these measurements show, or at least, can show about lubricant shear stresses. The data of Figure 21(a) have been manipulated, as previously described, to show inferred shear stress for both the inlet side of the measurement and the outlet side (Figures 22(a) and 22(b)). The two curves are considerably different. Further, this difference was very repeatable in the experiments.

The "inlet" shear stress curve, Figure 22(a) tends to show a higher peak and tends to conform to the Hertz contact pressure ellipse. This suggests that as the transducer enters into contact, the slot causes any lubricant to be depleted and only dry contact occurs. For this case, the shear stress would be a constant friction coefficient times the Hertz pressure.

The "outlet" shear stress, Figure 22(b), is measured as a result of the shear stress transducer being unloaded (in shear). For this case, lubricant could be trapped on the transducer by the normal elastohydrodynamic process. For this situation, the shear stress magnitude is reduced and spread out over a wide region.

The goal of these studies was to explore the feasibility of a shear stress transducer and the technique looks very promising. In future projects, it should be possible to refine this type of technique to obtain a new dimension in EHD measurements. These measurements will furnish critical inputs to understanding the lubricant behavior in concentrated contacts.

CONCLUSIONS

Two types of techniques for evaluating EHD lubrication have been presented in this report. The essence of the first technique has been described in previous reports and involves direct pressure and temperature measurements by the use of vapor-deposited transducer. In the current study, this technique was extended to include three-dimensional temperature-pressure mapping for the contact zone. The data are quite informative about the EHD contact and are to be evaluated, under separate ONR contract, by Dr. T. A. Dow at North Carolina State University.

The second technique discussed is a new concept for measuring traction distribution (or shear stresses) in the contact region. This technique incorporates two recently developed research tools,

(1) a sensitive (and stable) proximity probe,

(2) a computer-coupled oscilloscope.

The proximity probe allows for minor deflection of the shear transducer to be detected. The oscilloscope allows for the integrated traction measurements to be reduced to local shear stress. The preliminary measurements with the transducer indicate that it may be a powerful tool for EHD experiments.

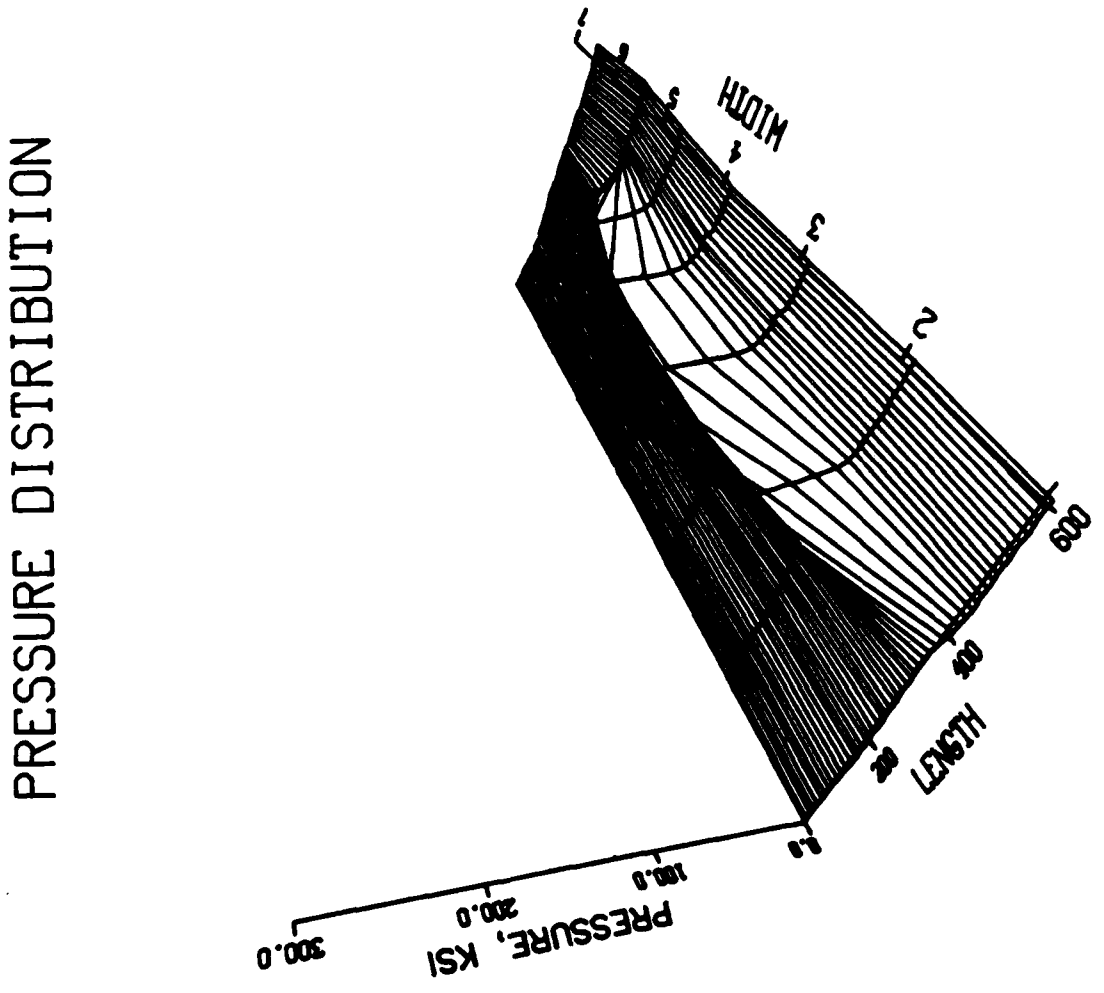

Figure 1A. Surface pressure and typical distribution for XRM-109F at 59C and 0.0 percent slip.

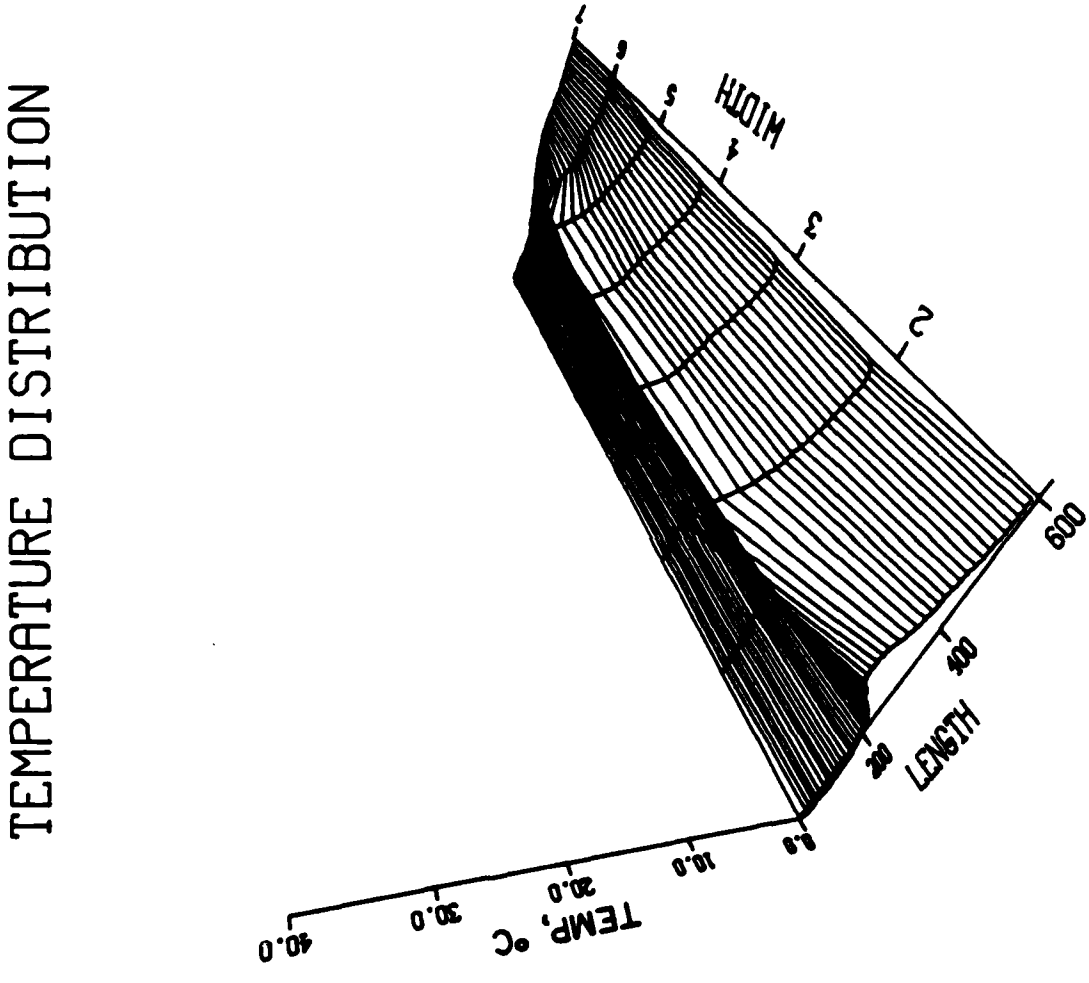

Figure 1B. Disk Load = 254 N (57 pounds)
Peak Pressure = 0.89 GPa (130 ksi)
Peak Temperature = 13C
Length Calibration = 3.12×10^{-3} mm/div (0.123 inch/div)
Width Calibration = 0.51 mm/div (0.020 inch/div)

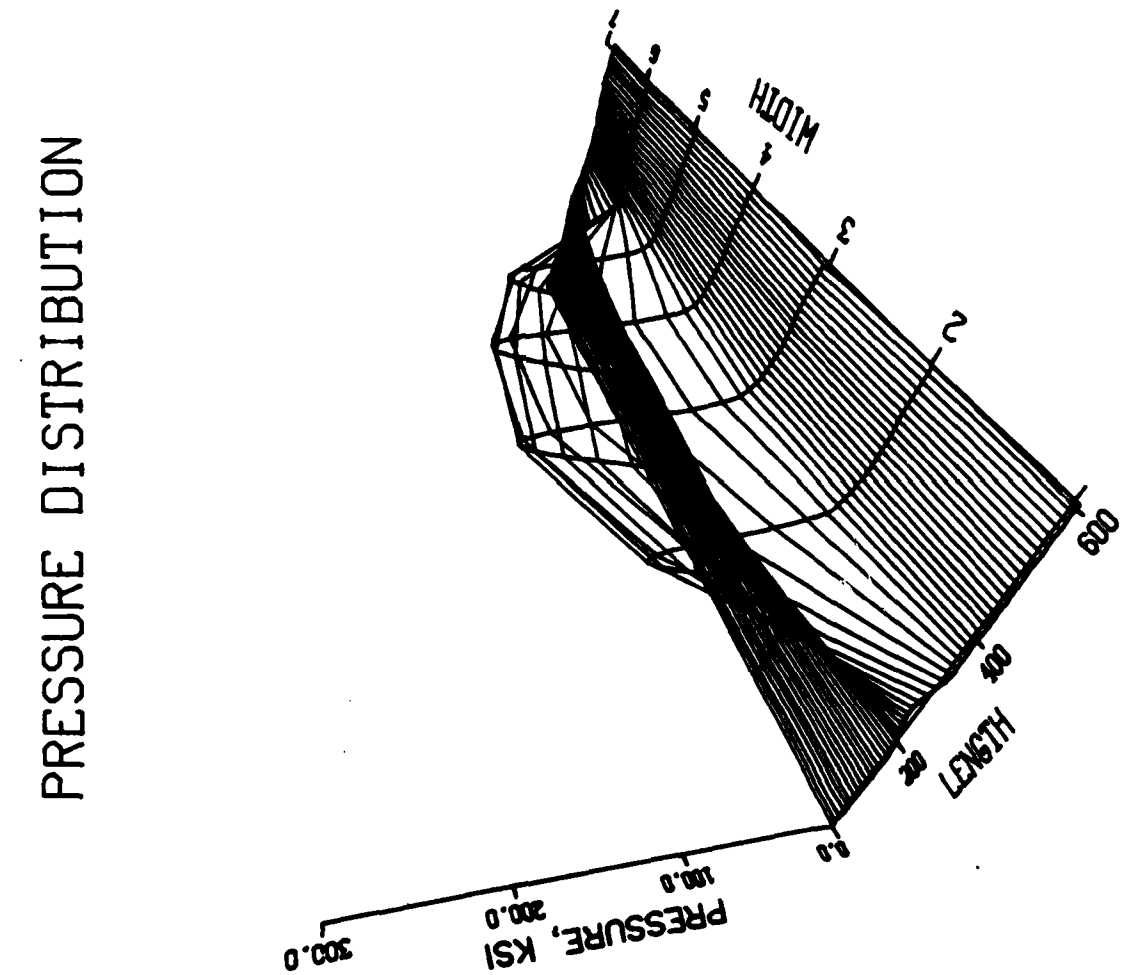

Figure 2A. Surface pressure and temperature distribution for XRM-109F at 59C and 0.0 percent slip.

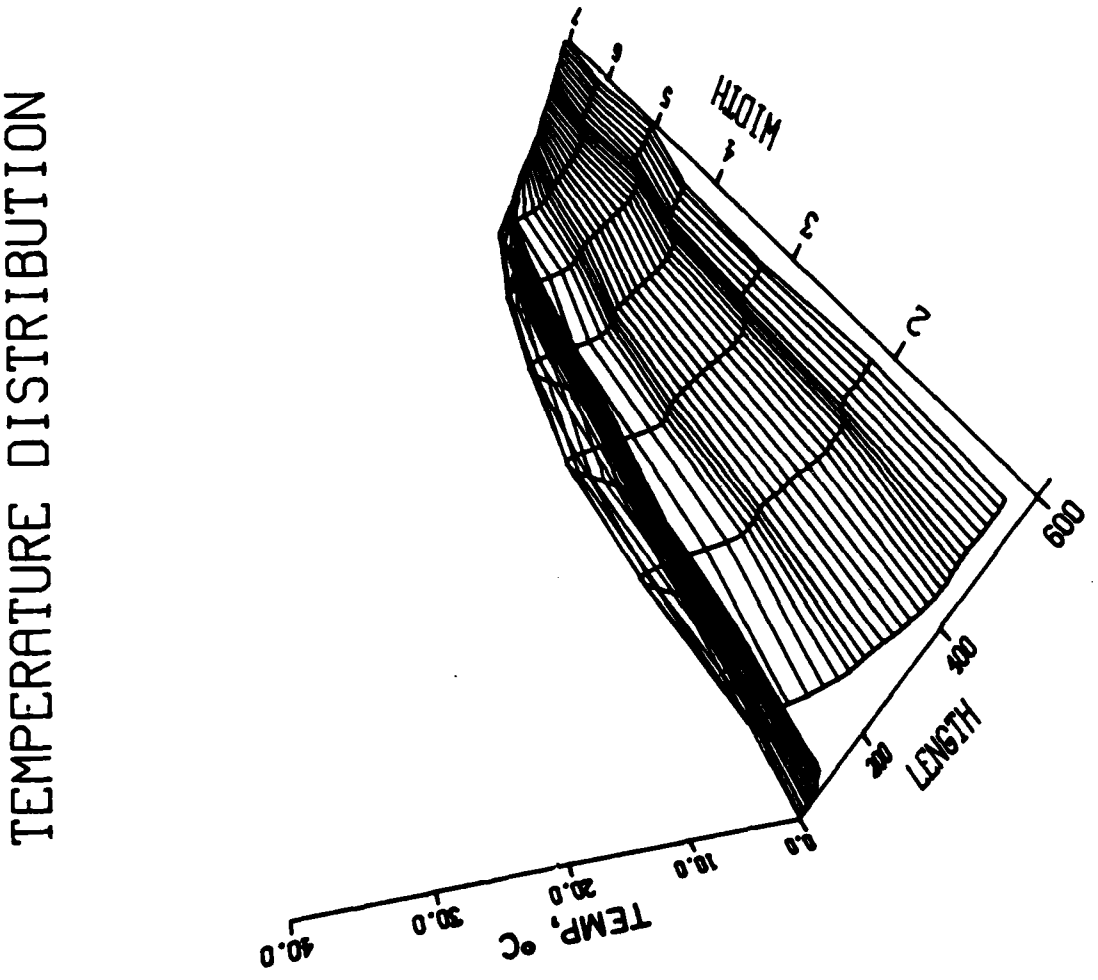

Figure 2B. Disk Load = 454 N (102 pounds)
Peak Pressure = 1.07 GPa (156 ksi)
Peak Temperature = 14C
Length Calibration = 3.12×10^{-3} mm/div (0.123 inch/div)
Width Calibration = 0.51 mm/div (0.020 inch/div)

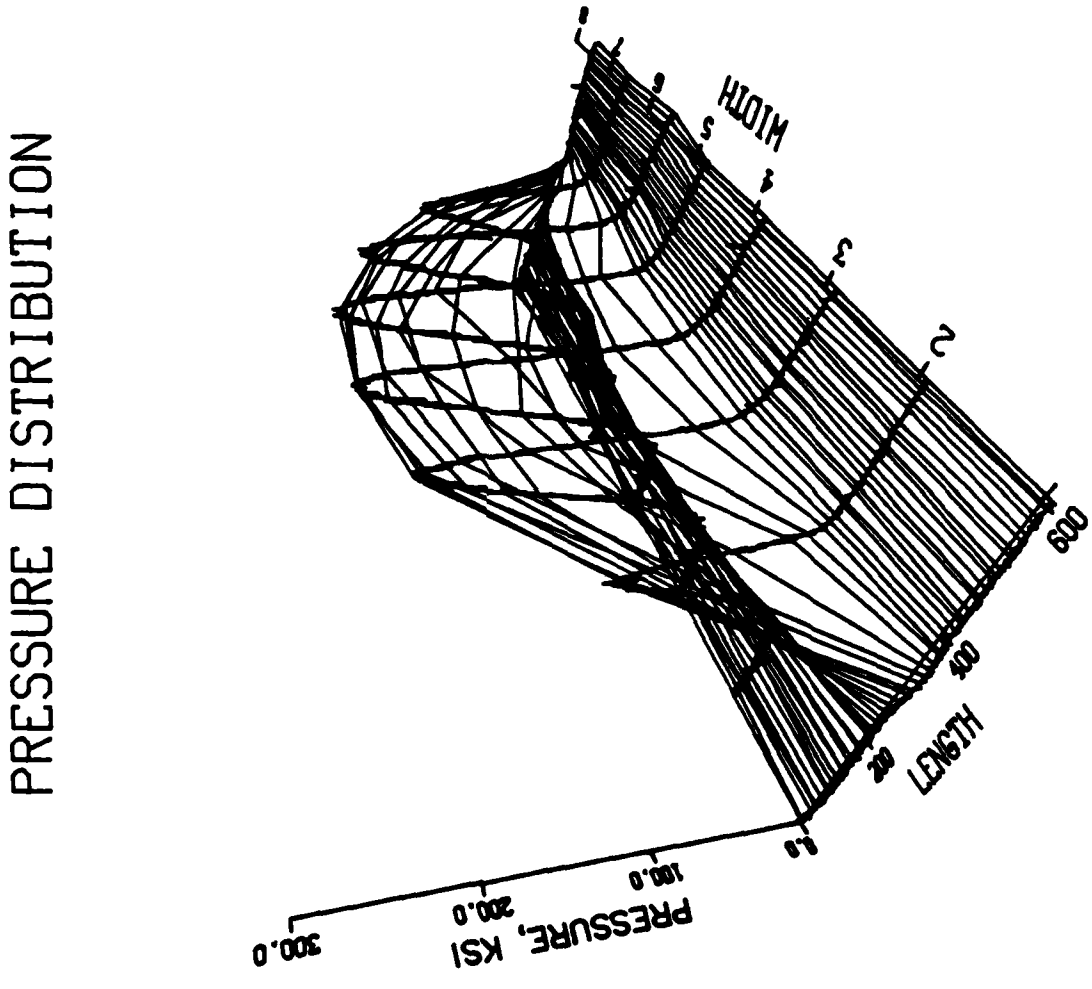

Figure 3A. Surface pressure and temperature distribution for XRM-109F at 59C and 0.0 percent slip.

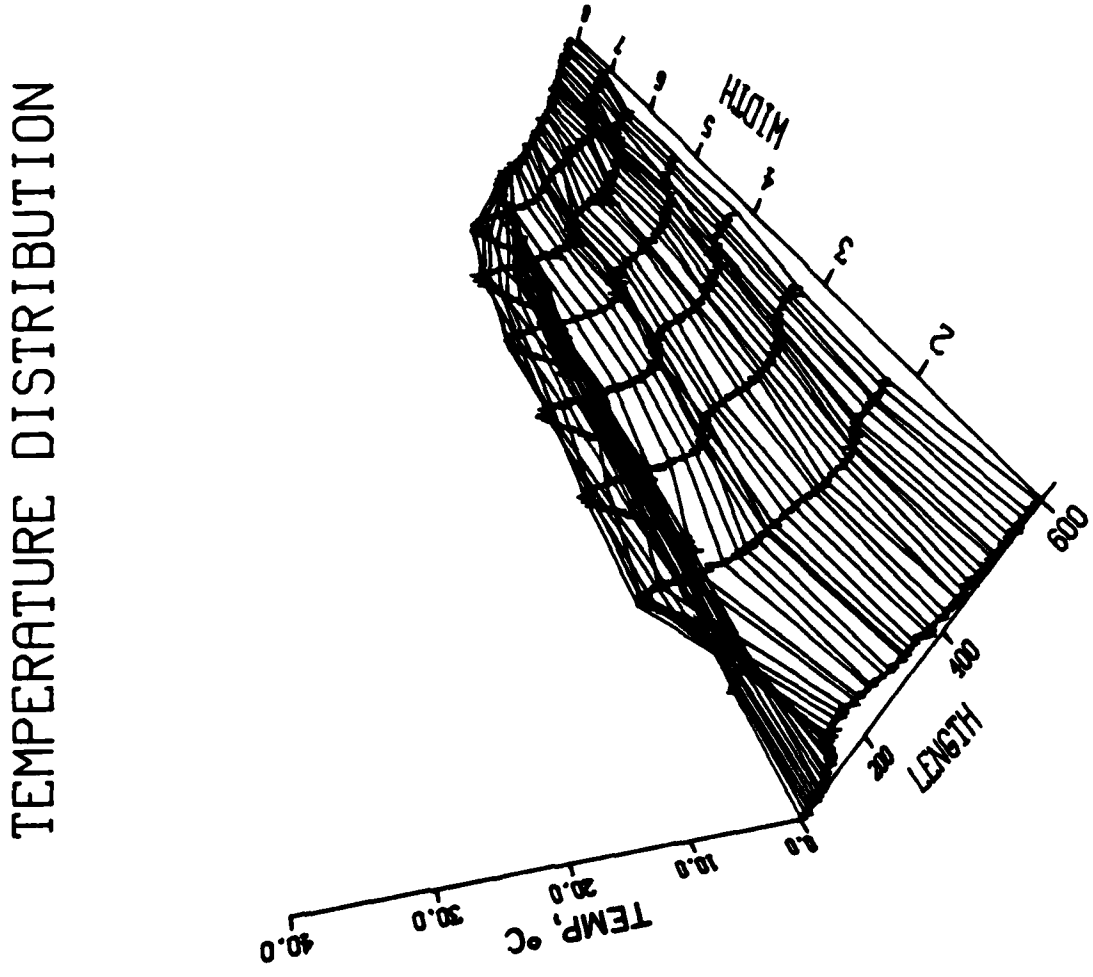

Figure 3B. Disk Load = 970 N (218 pounds)
Peak Pressure = 1.39 GPa (203 ksi)
Peak Temperature = 15C
Length Calibration = 3.12×10^{-3} mm/div (0.123 inch/div)
Width Calibration = 0.51 mm/div (0.020 inch/div)

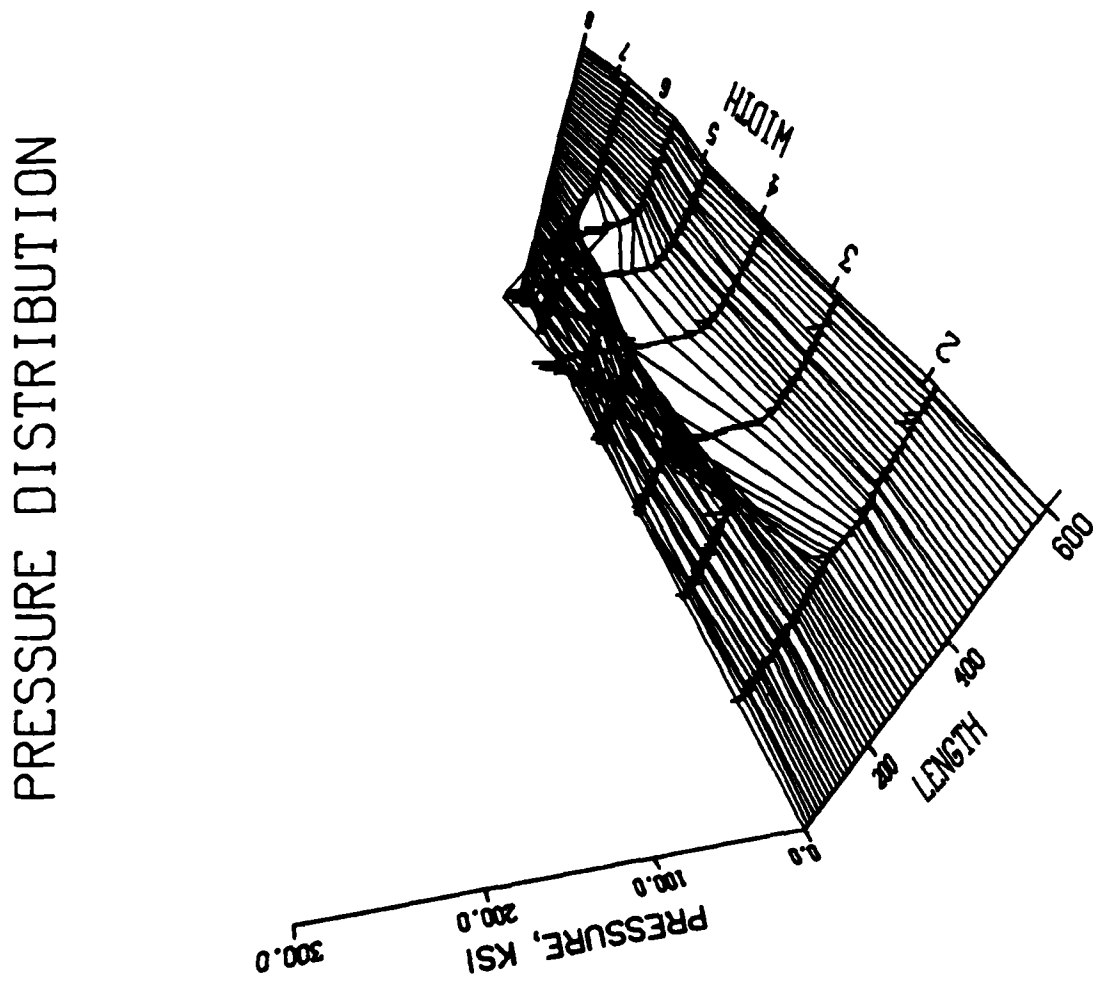

Figure 4A. Surface pressure and temperature distribution for XRM-109F at 58C and 5.8 percent slip.

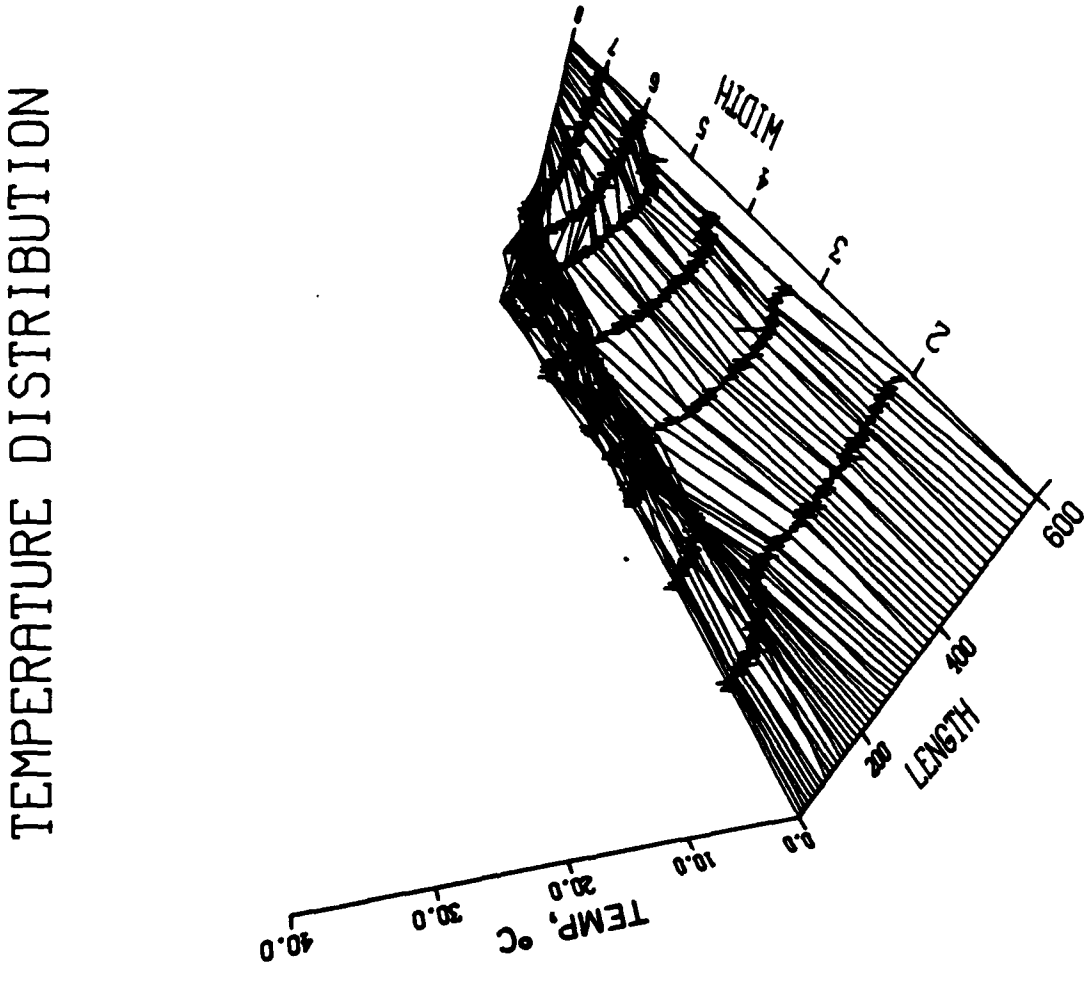

Figure 4B. Disk Load = 254 N (57 pounds)
Peak Pressure = 0.89 GPa (130 ksi)
Peak Temperature = 15 C
Length Calibration = 3.12×10^{-3} mm/div (0.123 inch/div)
Width Calibration = 0.51 mm/div (0.020 inch/div)

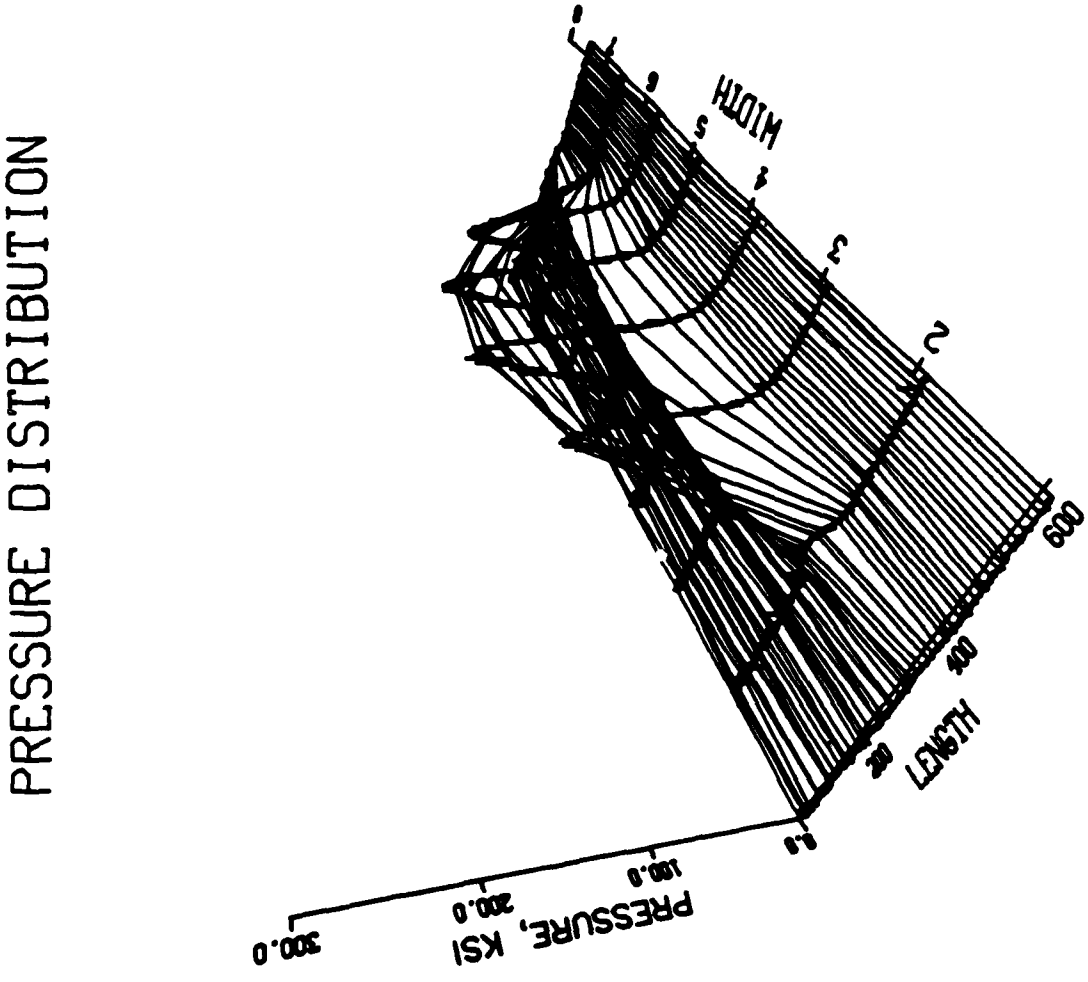

Figure 5A. Surface pressure and temperature distribution for XRM-109F at 58C and 5.3 percent slip.

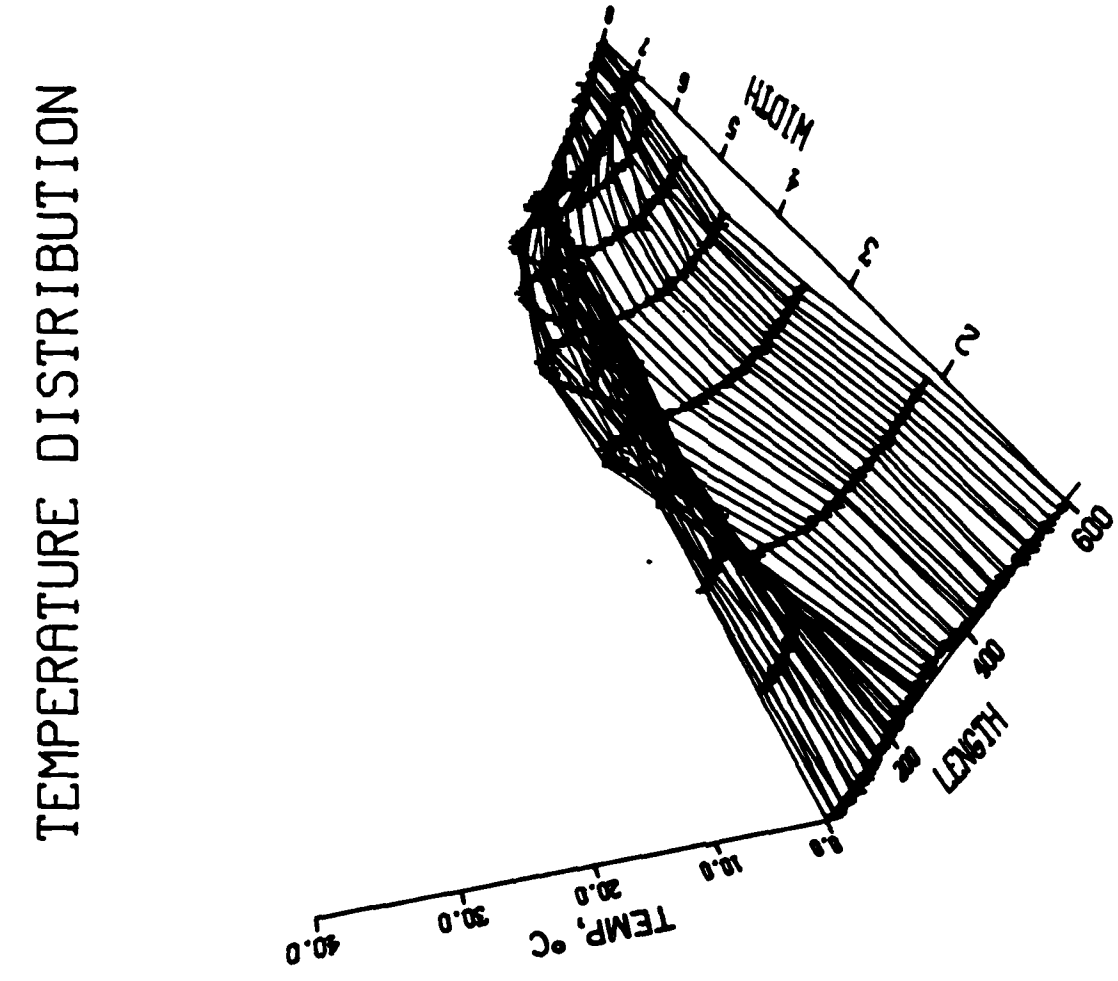

Figure 5B. Disk Load = 454 N (102 pounds)
Peak Pressure = 1.08 GPa (156 ksi)
Peak Temperature = 18C
Length Calibration = 3.12×10^{-3} mm/div (0.123 inch/div)
Width Calibration = 0.51 mm/div (0.020 inch/div)

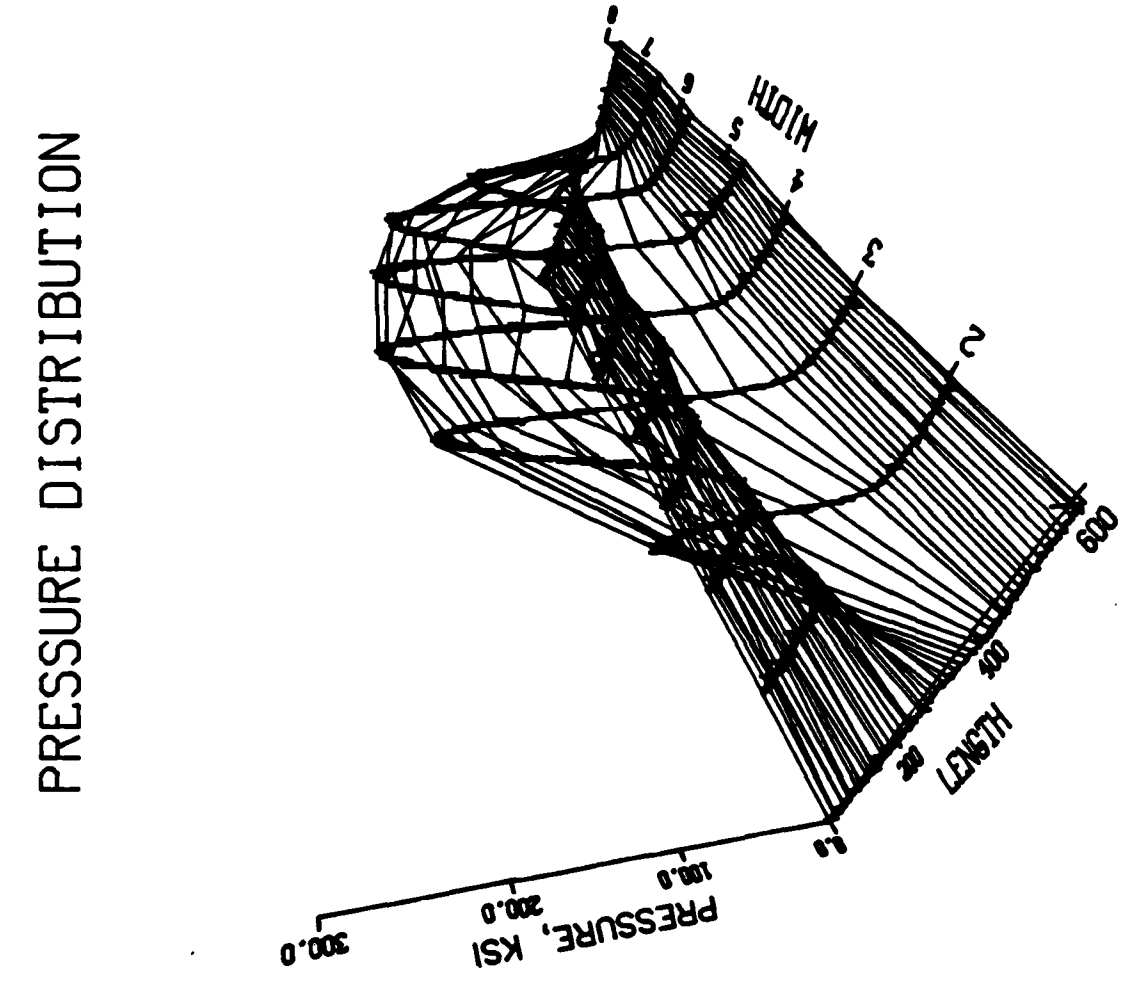

Figure 6A. Surface pressure and temperature distribution for XRM-109F at 63C and 6.2 percent slip.

TEMPERATURE DISTRIBUTION

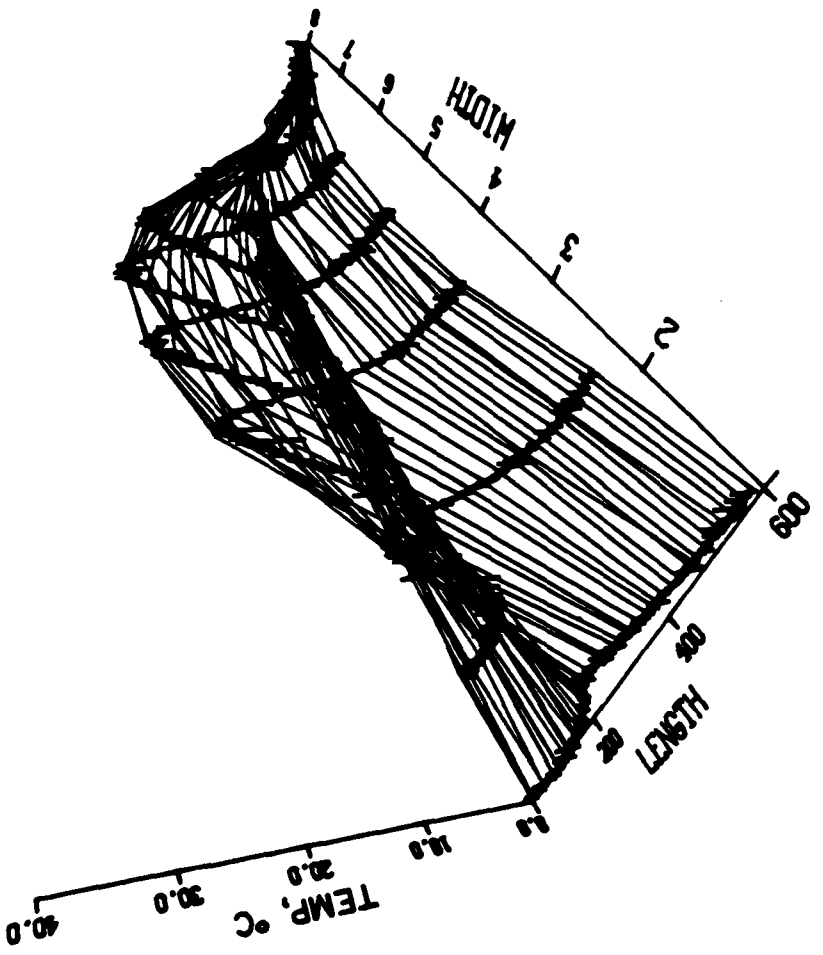

Figure 6B. Disk Load = 970 N (218 pounds)
Peak Pressure = 1.39 GPa (203 ksi)
Peak Temperature = 28C
Length Calibration = 3.12×10^{-3} mm/div (0.123 inch/div)
Width Calibration = 0.51 mm/div (0.020 inch/div)

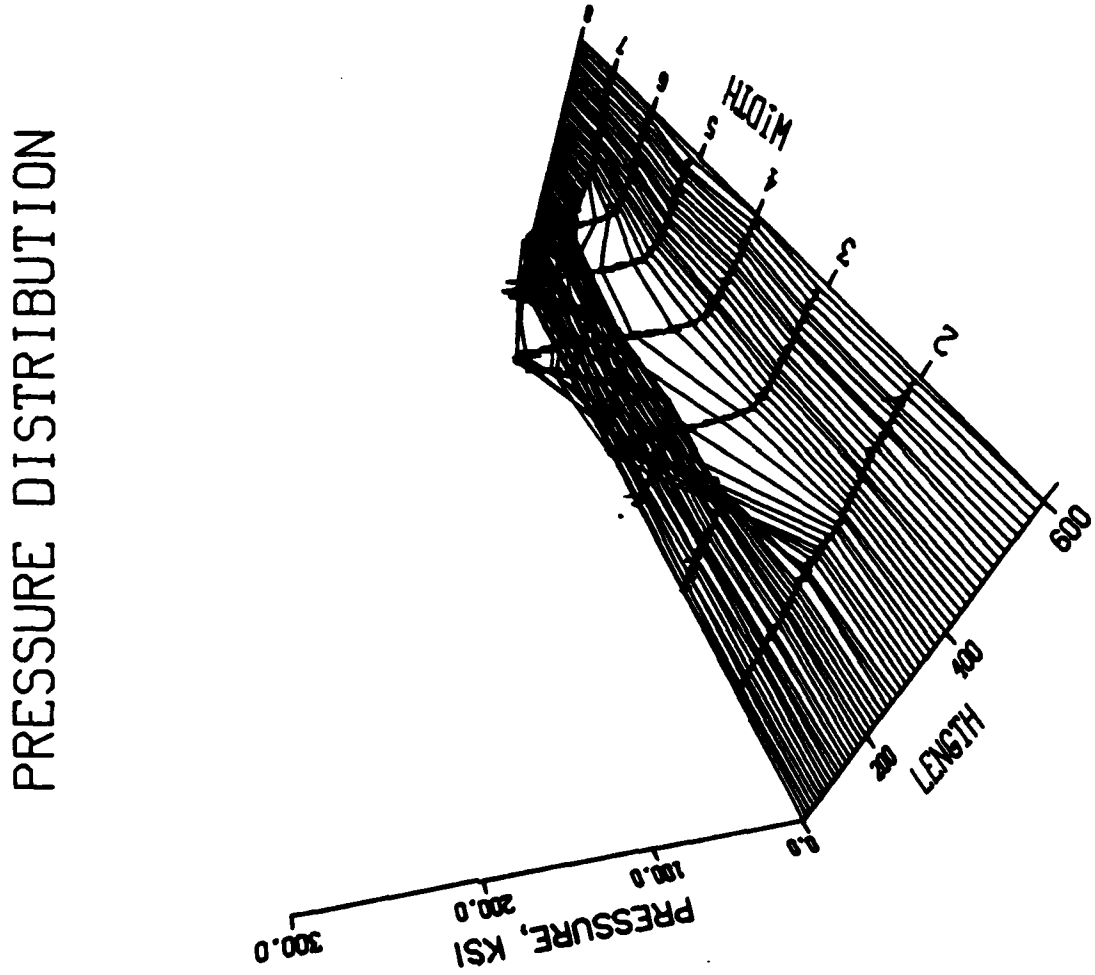

Figure 7A. Surface pressure and temperature distribution for OS-124 at 75C and 0.0 percent slip.

TEMPERATURE DISTRIBUTION

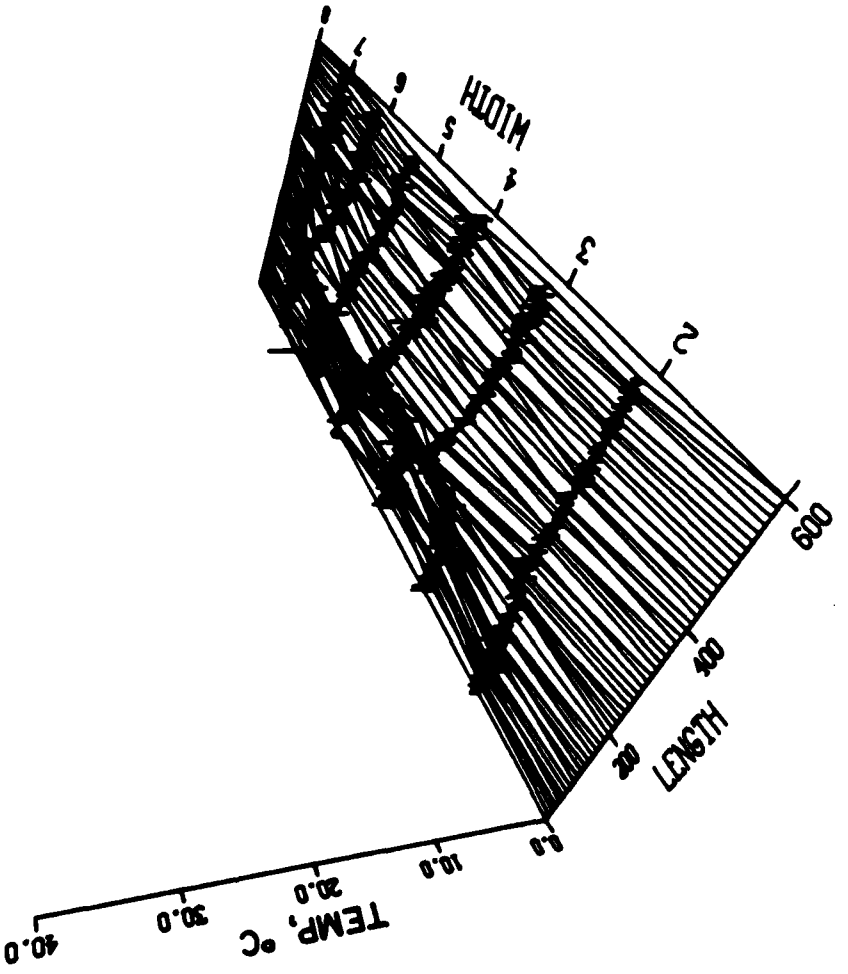

Figure 7B. Disk Load = 254 N (57 pounds)
Peak Pressure = 0.89 GPa (130 ksi)
Peak Temperature = 7C
Length Calibration = 3.12×10^{-3} mm/div (0.123 inch/div)
Width Calibration = 0.51 mm/div (0.020 inch/div)

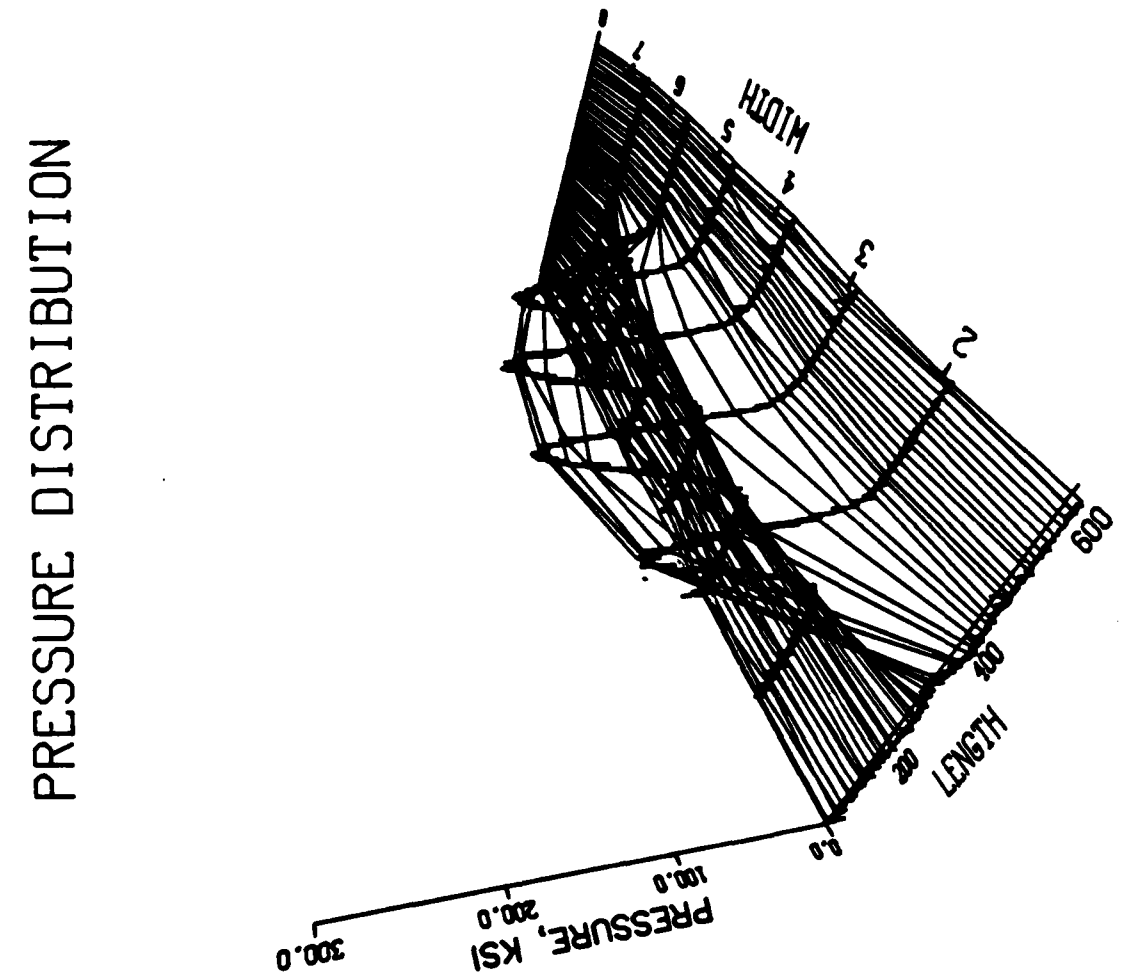

Figure 8A. Surface pressure and temperature distribution for OS-124 at 72C and 0.0 percent slip.

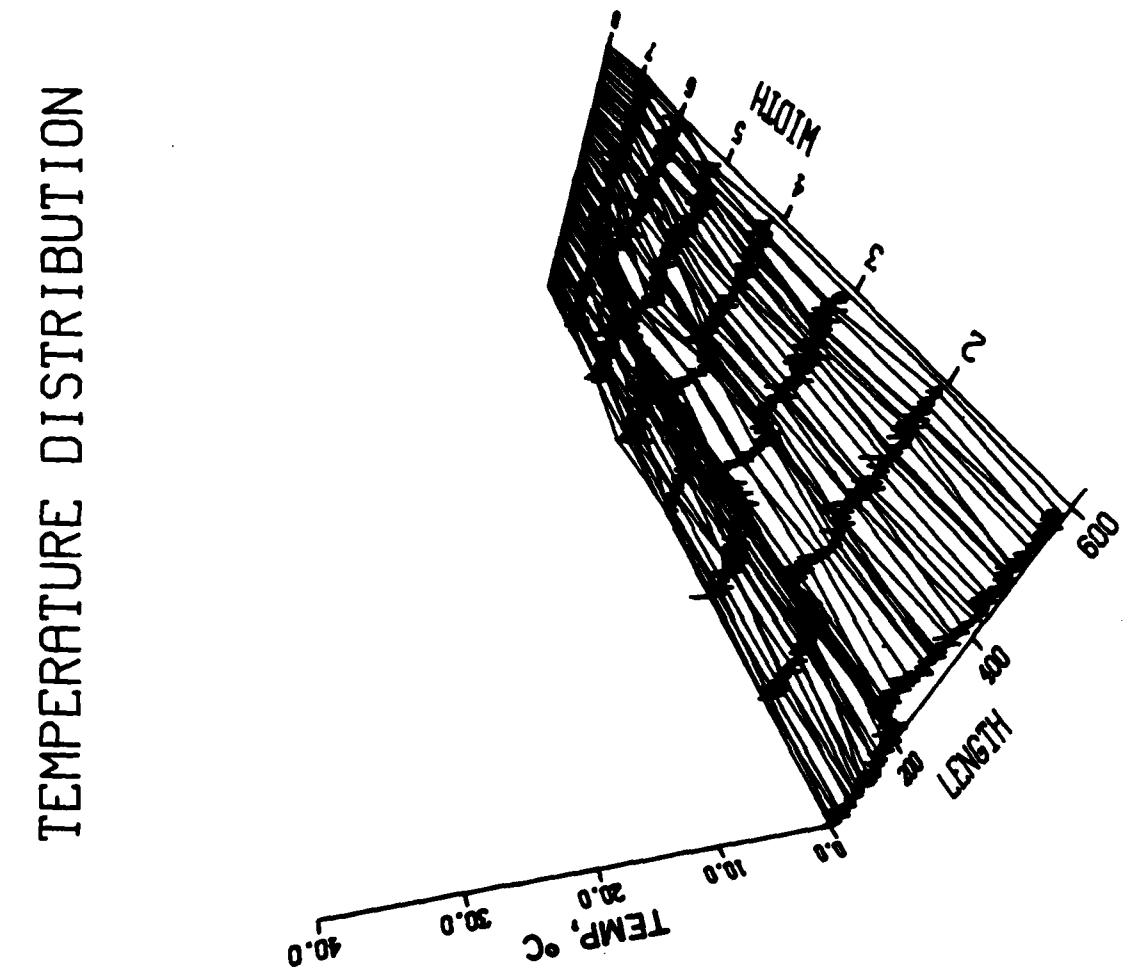

Figure 8B. Disk Load = 454 N (102 pounds)
Peak Pressure = 1.07 GPa (156 ksi)
Peak Temperature = 5C
Length Calibration = 3.12×10^{-3} mm/div (0.123 inch/div)
Width Calibration = 0.51 mm/div (0.020 inch/div)

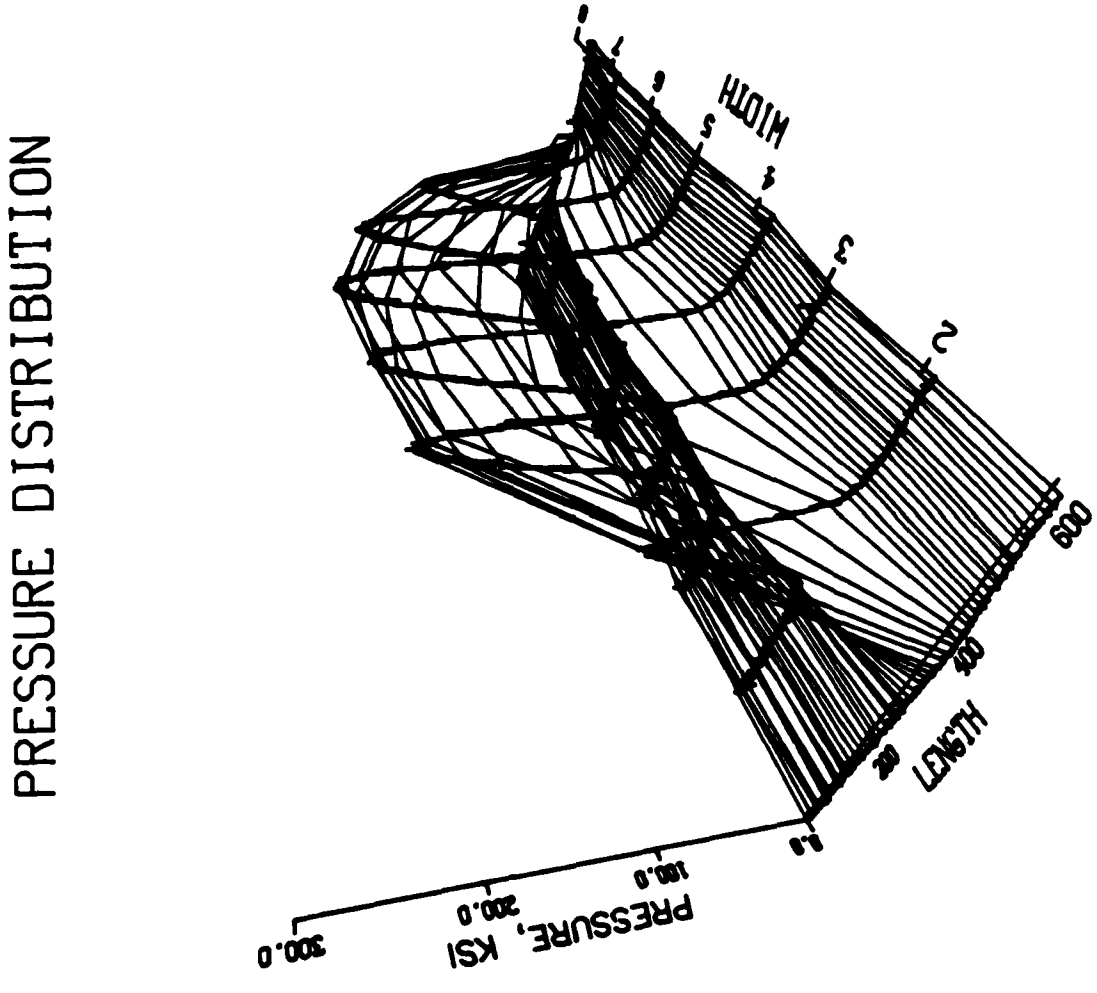

Figure 9A. Surface pressure and temperature distribution for OS-124 at 72C and 0.0 percent slip.

TEMPERATURE DISTRIBUTION

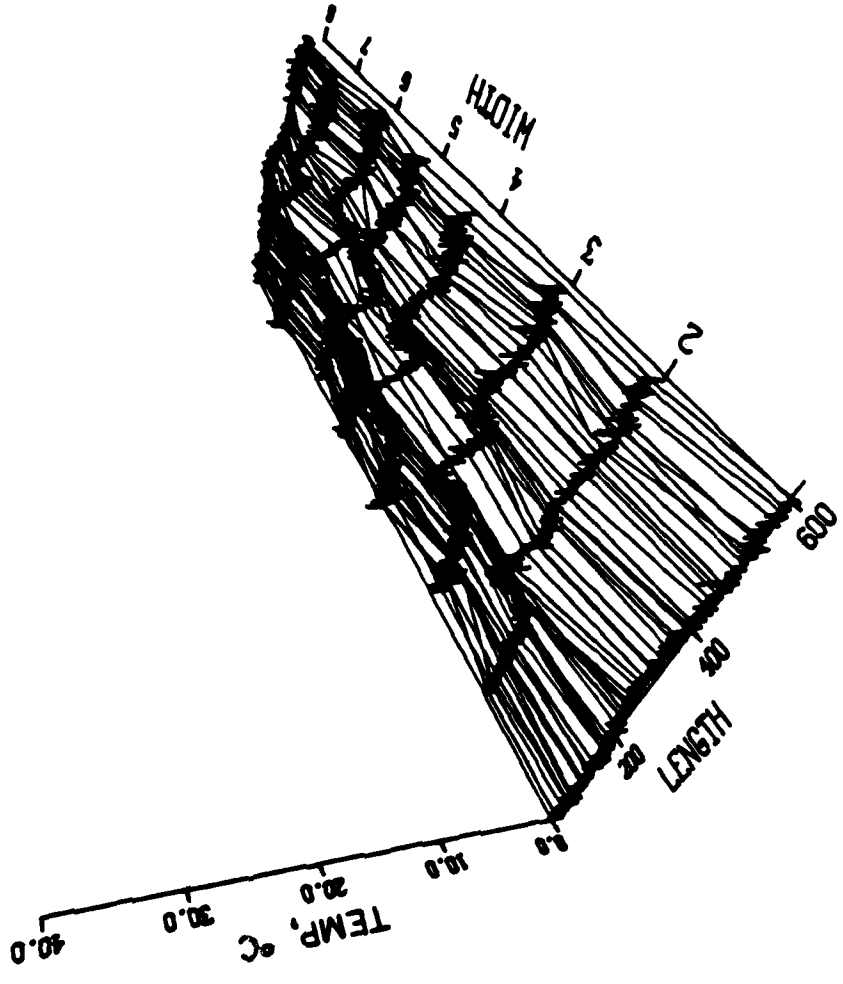

Figure 9B. Disk Load = 970 N (218 pounds)
Peak Pressure = 1.39 GPa (203 ksi)
Peak Temperature = 5C
Length Calibration = 3.12×10^{-3} mm/div (0.123 inch/div)
Width Calibration = 0.51 mm/div (0.020 inch/div)

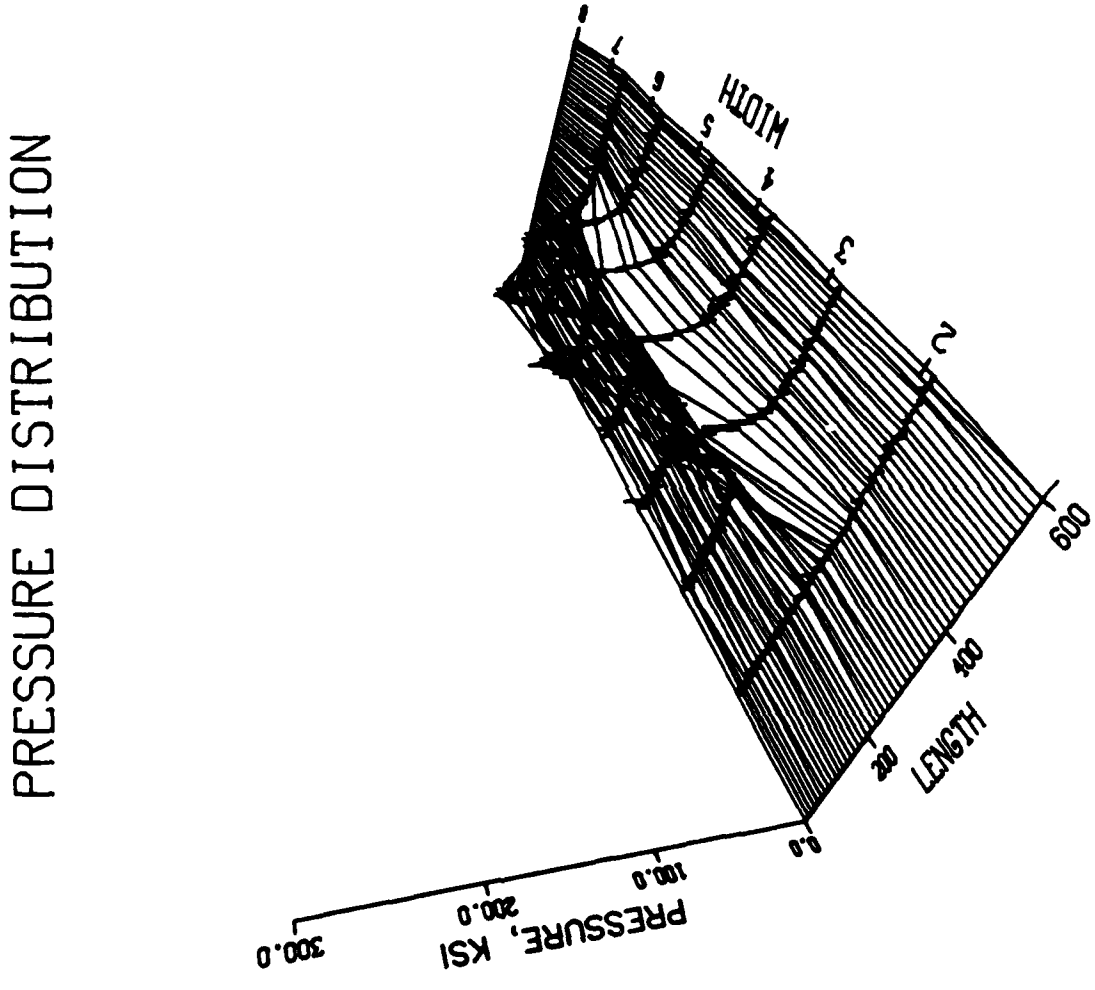

Figure 10A. Surface pressure and temperature distribution for OS-124 at 77C and 5.9 percent slip.

TEMPERATURE DISTRIBUTION

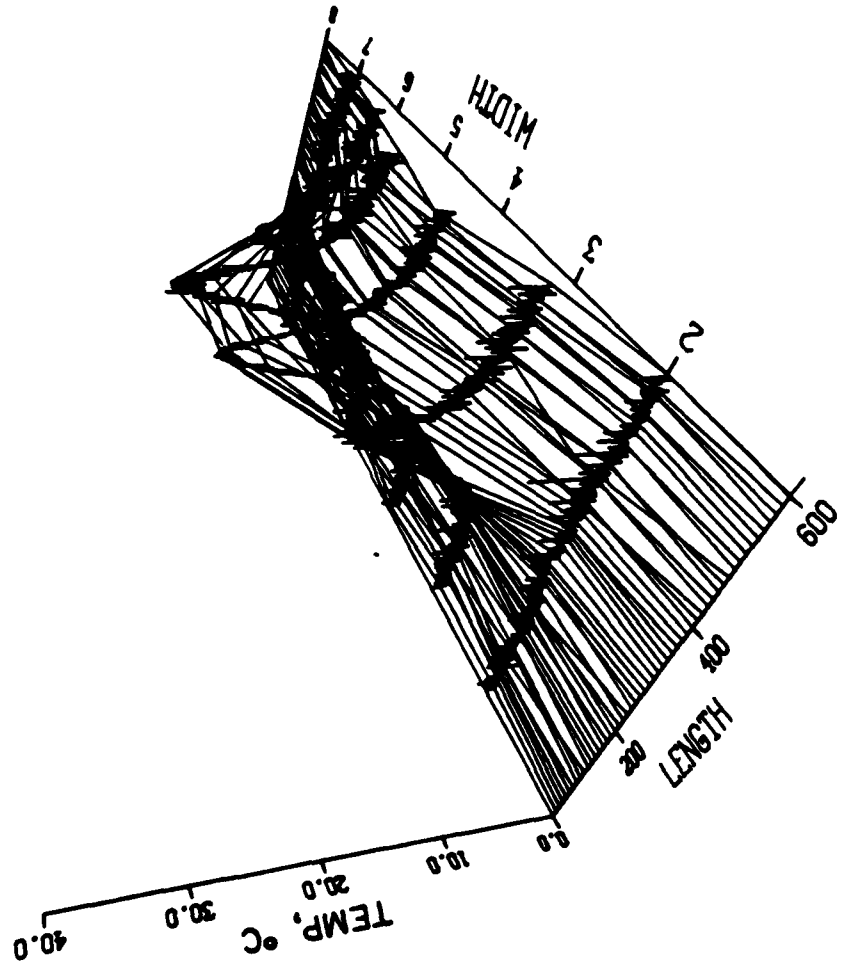

Figure 10B. Disk Load = 254 N (57 pounds)
Peak Pressure = 0.89 GPa (130 ksi)
Peak Temperature = 24C
Length Calibration = 3.12×10^{-3} mm/div (0.123 inch/div)
Width Calibration = 0.51 mm/div (0.020 inch/div)

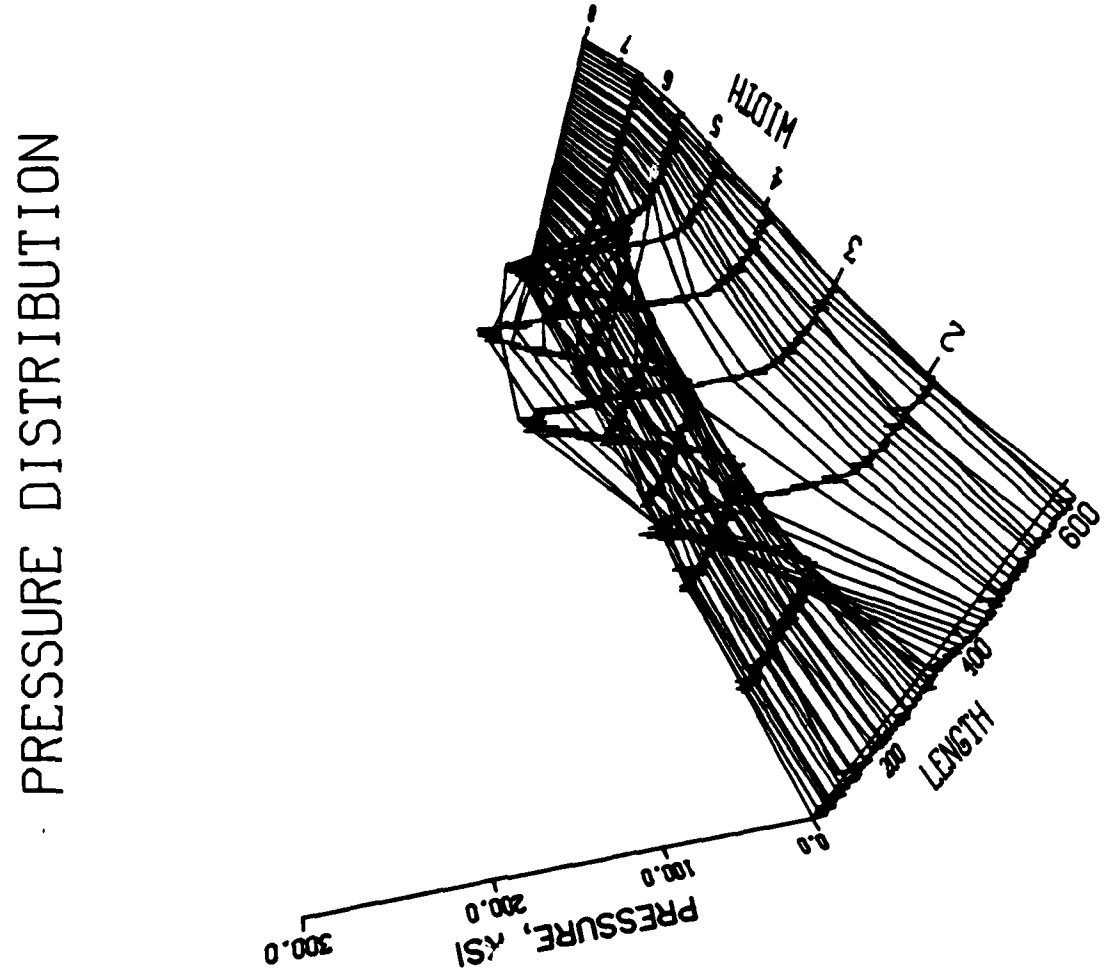

Figure 11A. Surface pressure and temperature distribution for OS-124 at 76C and 4.4 percent slip.

TEMPERATURE DISTRIBUTION

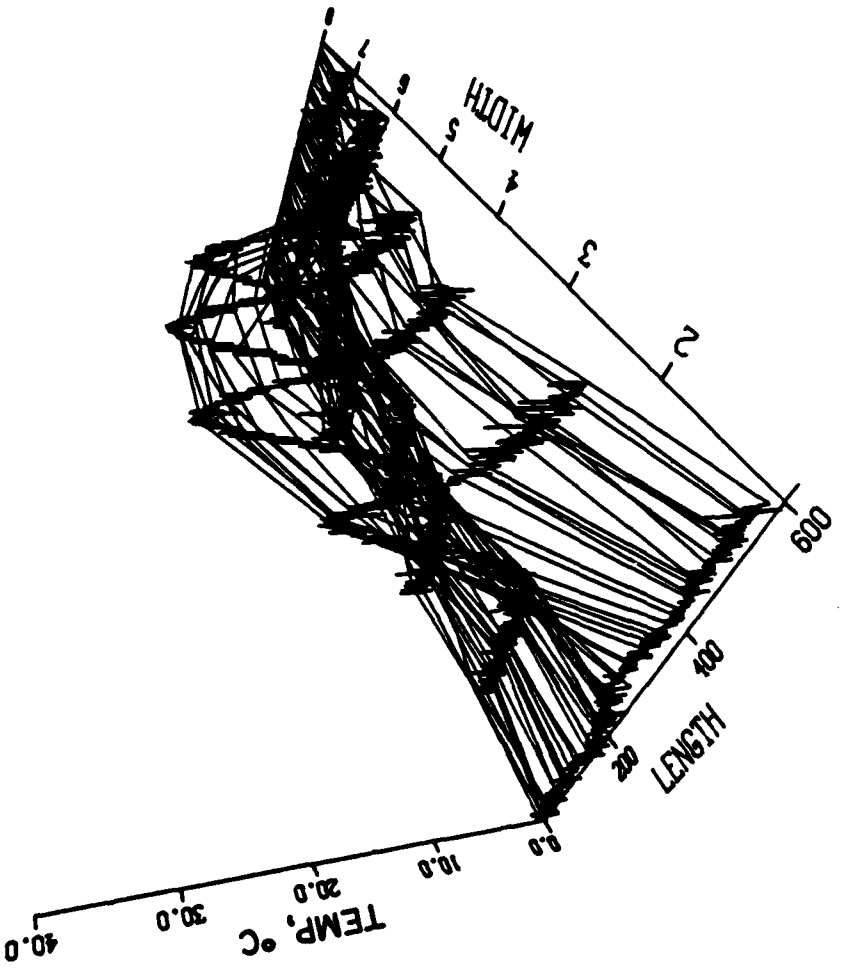

Figure 11A. Disk Load = 454 N (102 pounds)
Peak Pressure = 1.07 GPa (156 ksi)
Peak Temperature = 27C
Length Calibration = 3.12×10^{-3} mm/div (0.123 inch/div)
Width Calibration = 0.51 mm/div (0.020 inch/div)

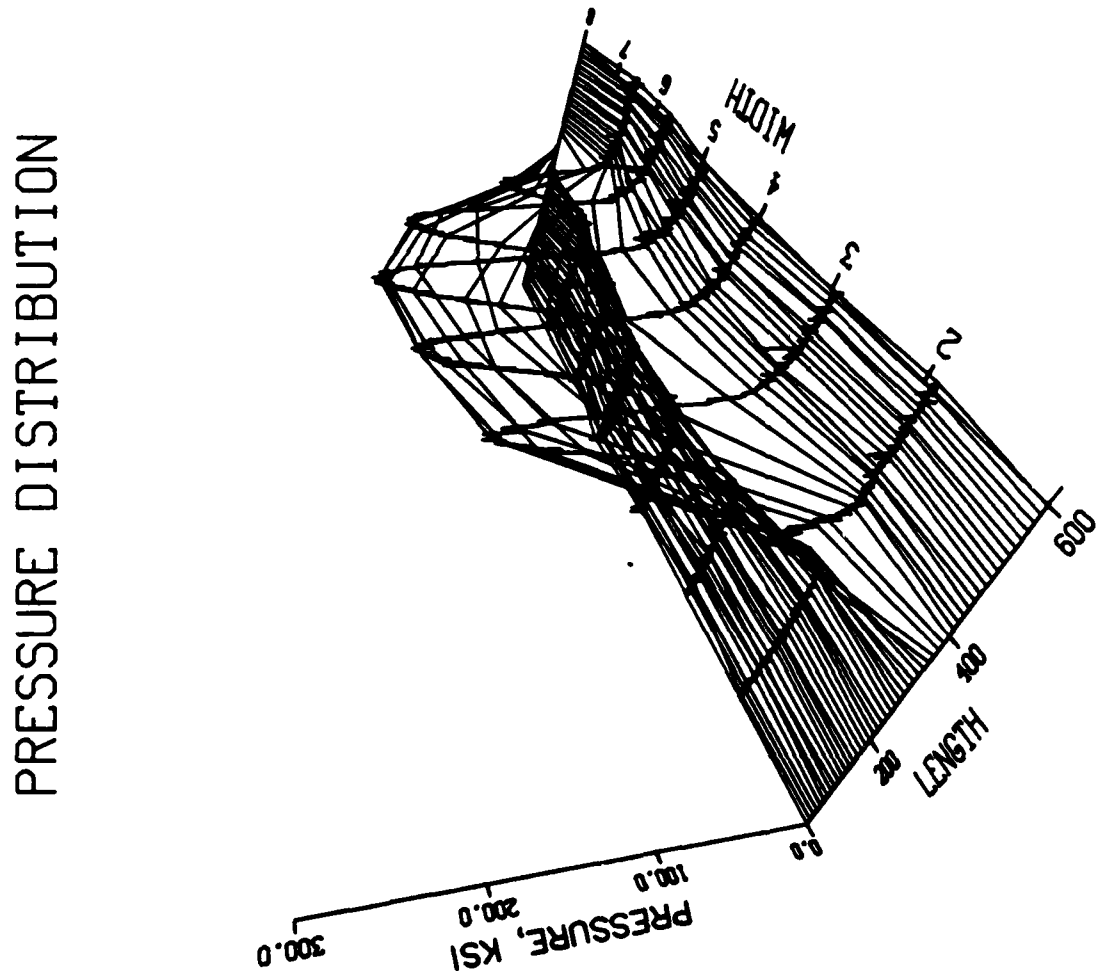

Figure 12A. Surface pressure and temperature distribution for OS-124 at 81C and 3.5 percent slip.

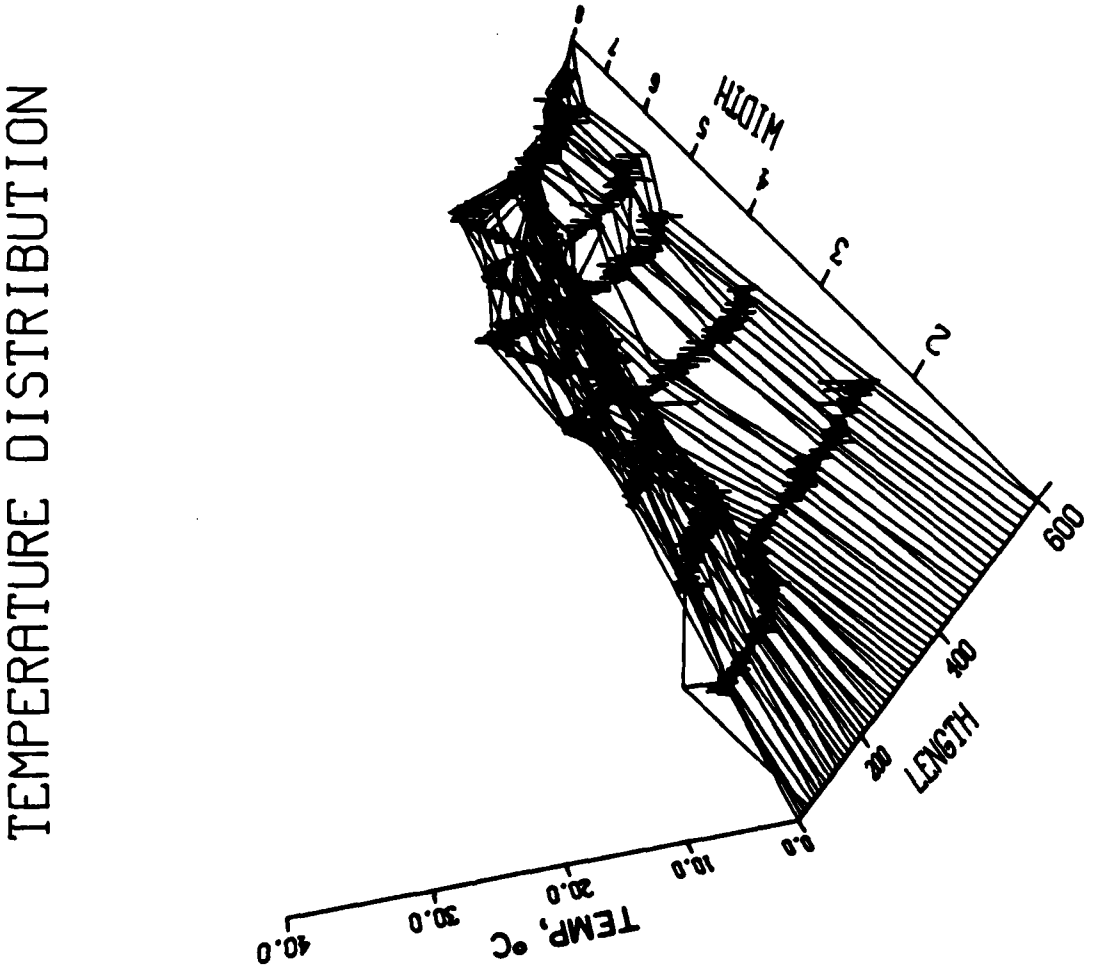

Figure 12B. Disk Load = 658 N (148 pounds)
Peak Pressure = 1.22 GPa (177 ksi)
Peak Temperature = 20C
Length Calibration = 3.12×10^{-3} mm/div (0.123 inch/div)
Width Calibration = 0.51 mm/div (0.020 inch/div)

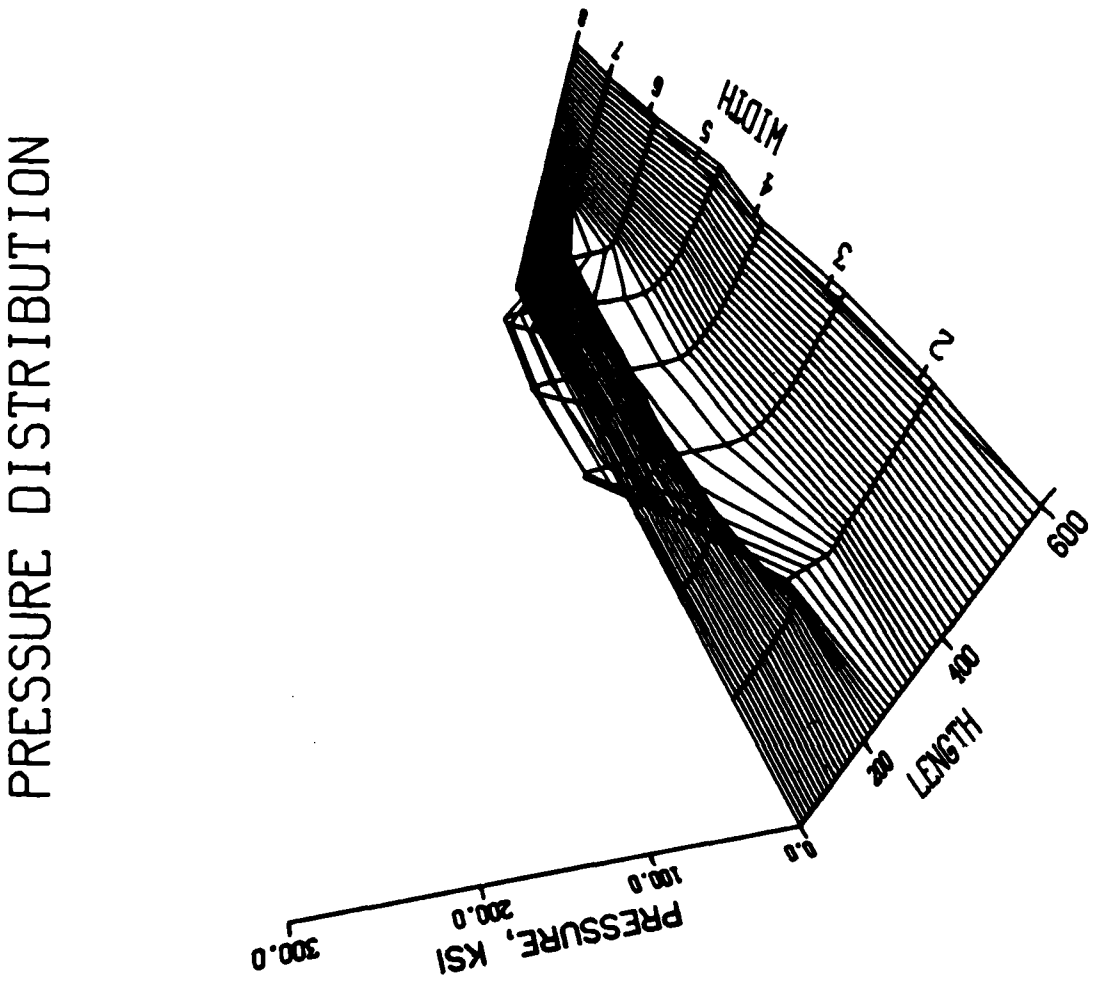

Figure 13A. Surface pressure and temperature distribution for Santotrac 50 at 24C and 0.0 percent slip.

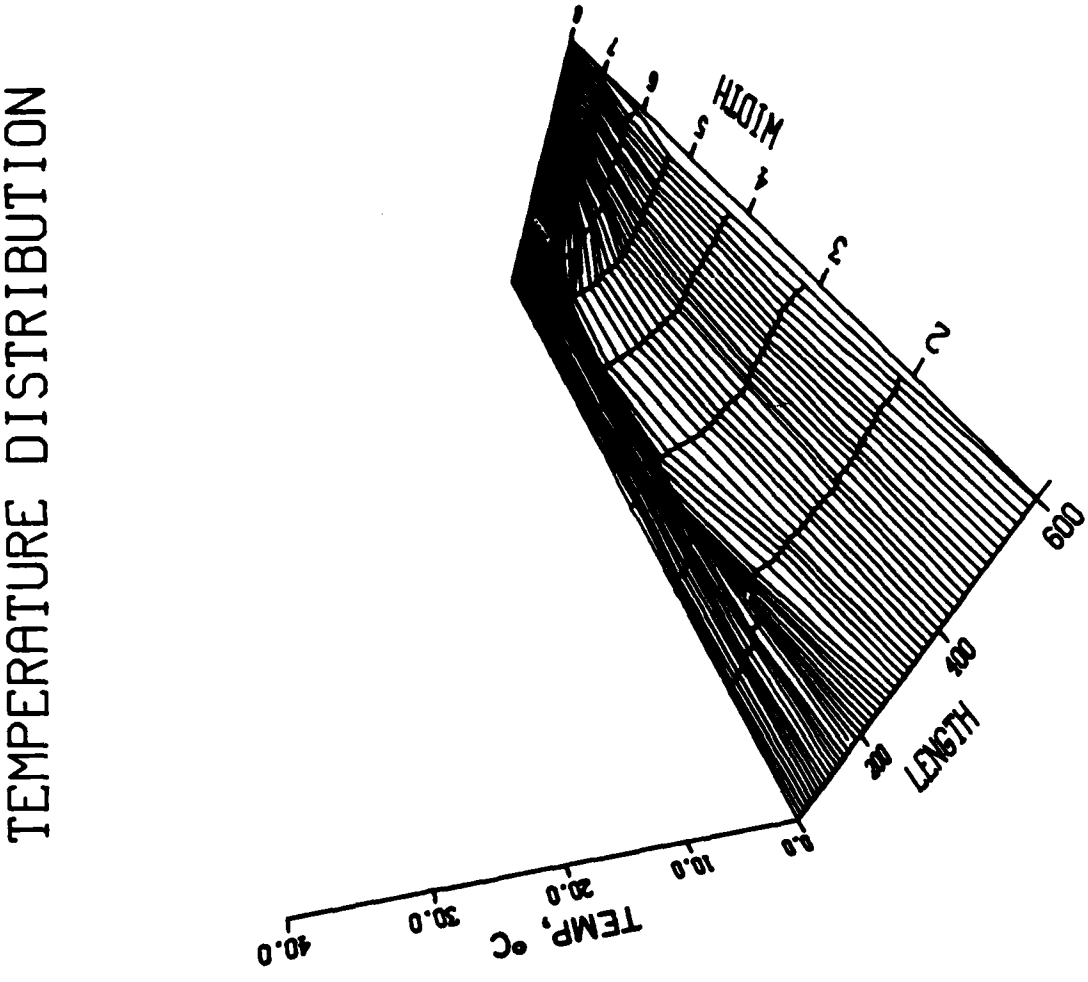

Figure 13B. Disk Load = 254 N (57 pounds)
Peak Pressure = 0.89 GPa (130 ksi)
Peak Temperature = 9C
Length Calibration = 3.12×10^{-3} mm/div (0.123 inch/div)
Width Calibration = 0.51 mm/div (0.020 inch/div)

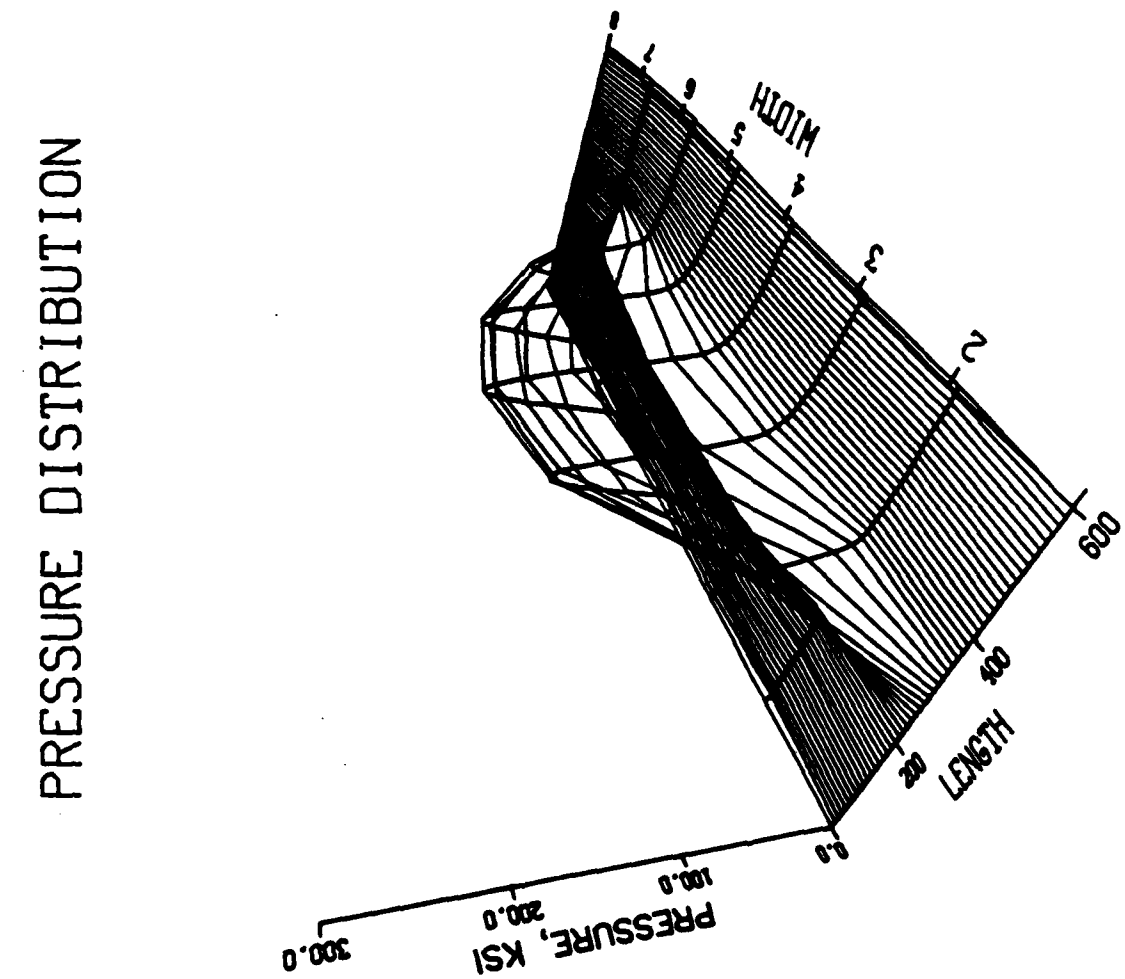

Figure 14A. Surface pressure and temperature distribution for Santotrac 50 at 24C and 0.0 percent slip.

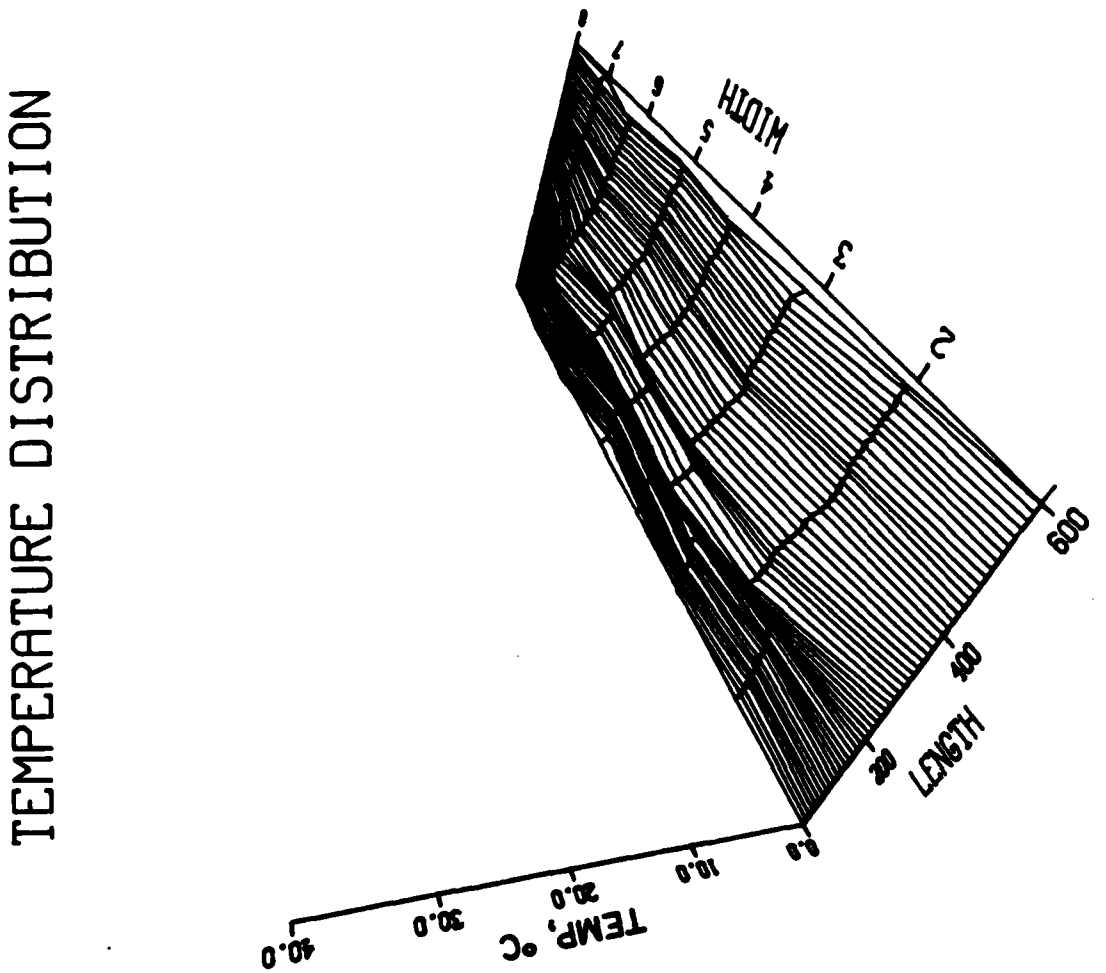

Figure 14B. Disk Load = 454 N (102 pounds)
Peak Pressure = 1.07 GPa (156 ksi)
Peak Temperature = 6C
Length Calibration = 3.12×10^{-3} mm/div (0.123 inch/div)
Width Calibration = 0.51 mm/div (0.020 inch/div)

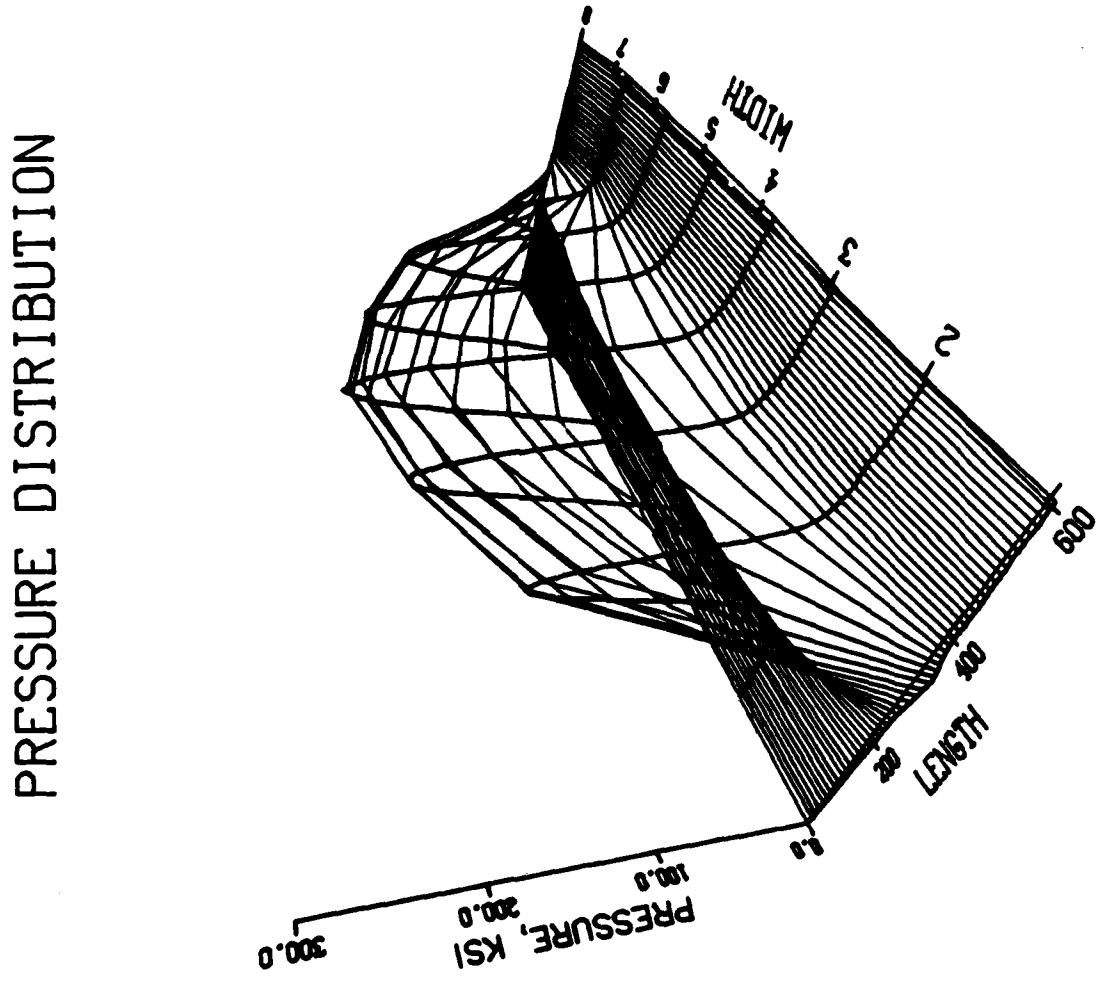

Figure 15A. Surface pressure and temperature distribution for Santotrac 50 at 24C and 0.0 percent slip.

TEMPERATURE DISTRIBUTION

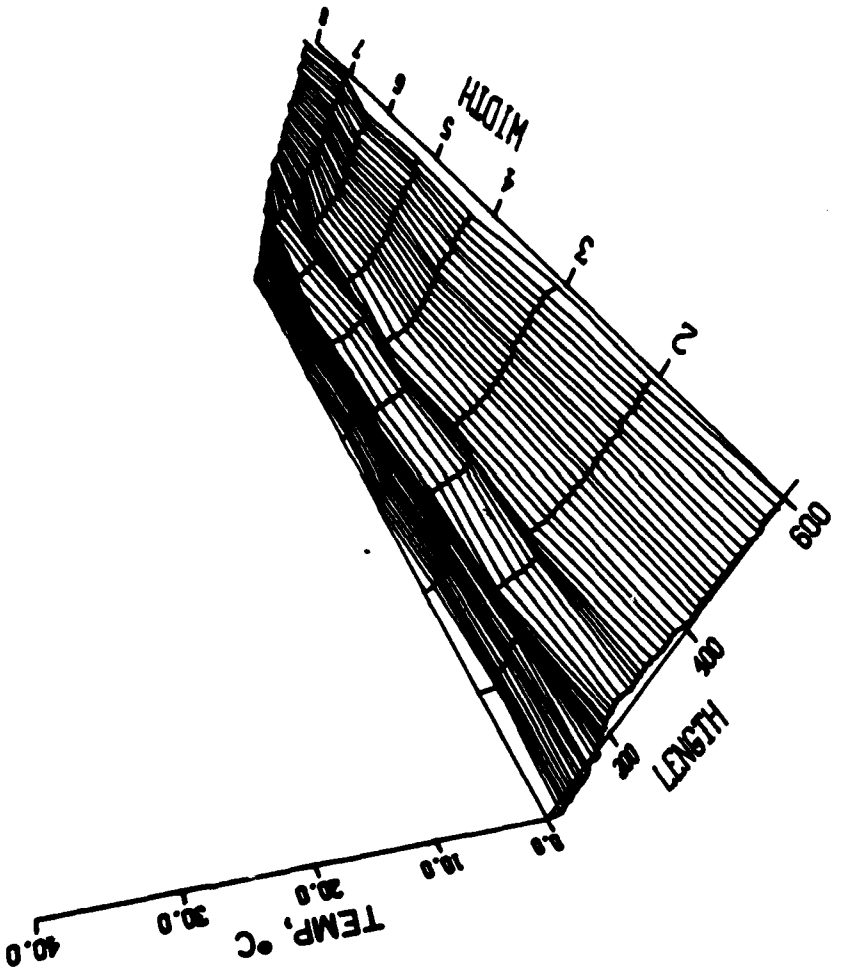

Figure 15B. Disk Load = 970 N (218 pounds)
Peak Pressure = 1.39 GPa (203 ksi)
Peak Temperature = 6.3C
Length Calibration = 3.12×10^{-3} mm/div (0.123 inch/div)
Width Calibration = 0.51 mm/div (0.020 inch/div)

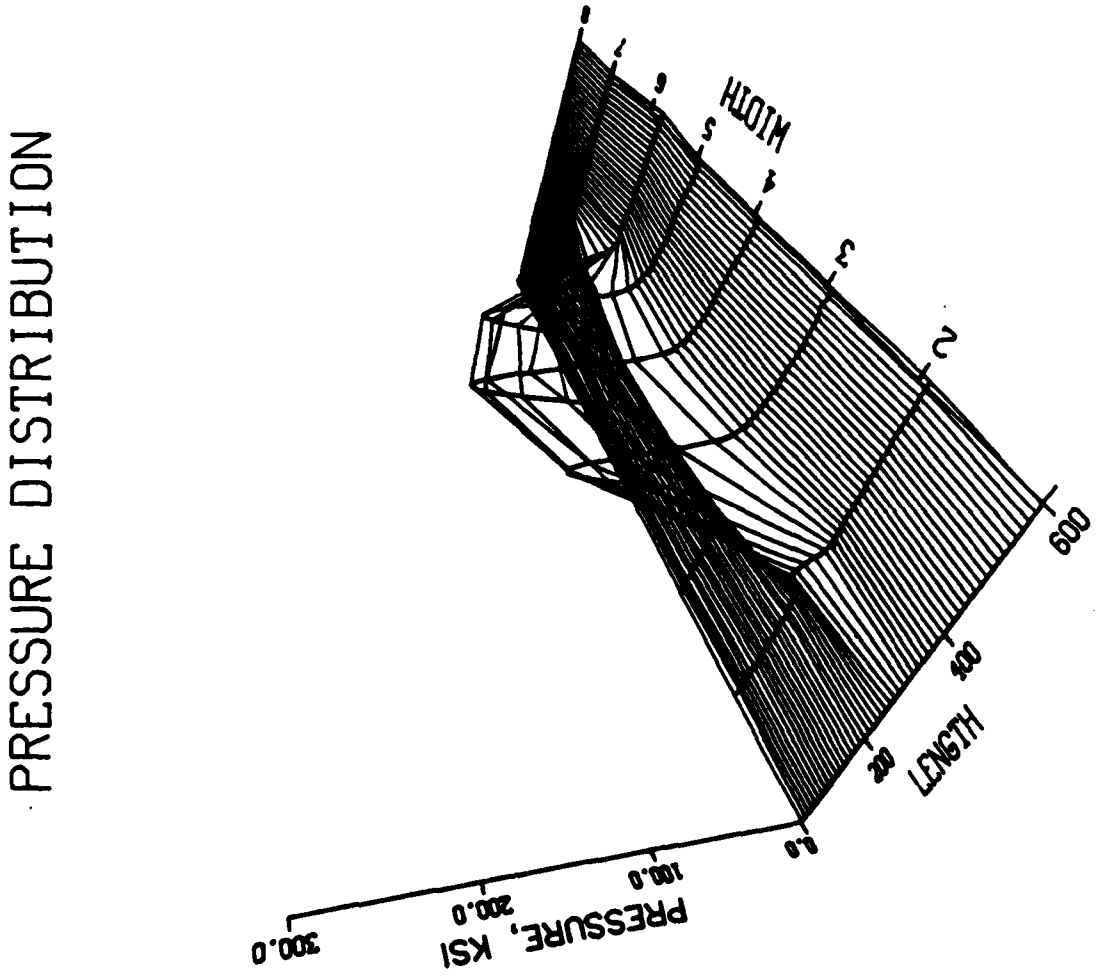

Figure 16A. Surface pressure and temperature distribution for Santotrac 50 at 27C and 5.5 percent slip.

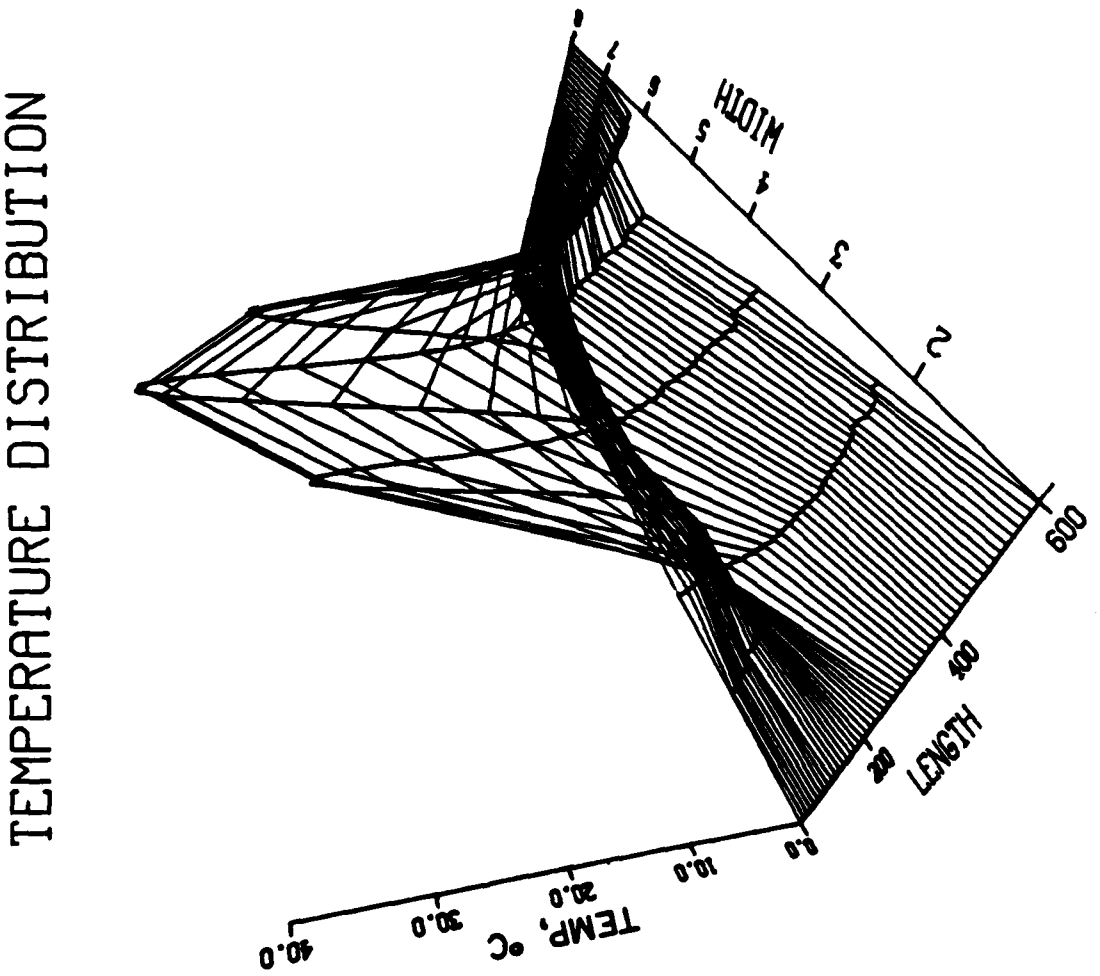

Figure 16B. Disk Load = 254 N (57 pounds)
Peak Pressure = 0.89 GPa (130 ksi)
Peak Temperature = 50C
Length Calibration = 3.12×10^{-3} mm/div (0.123 inch/div)
Width Calibration = 0.51 mm/div (0.020 inch/div)

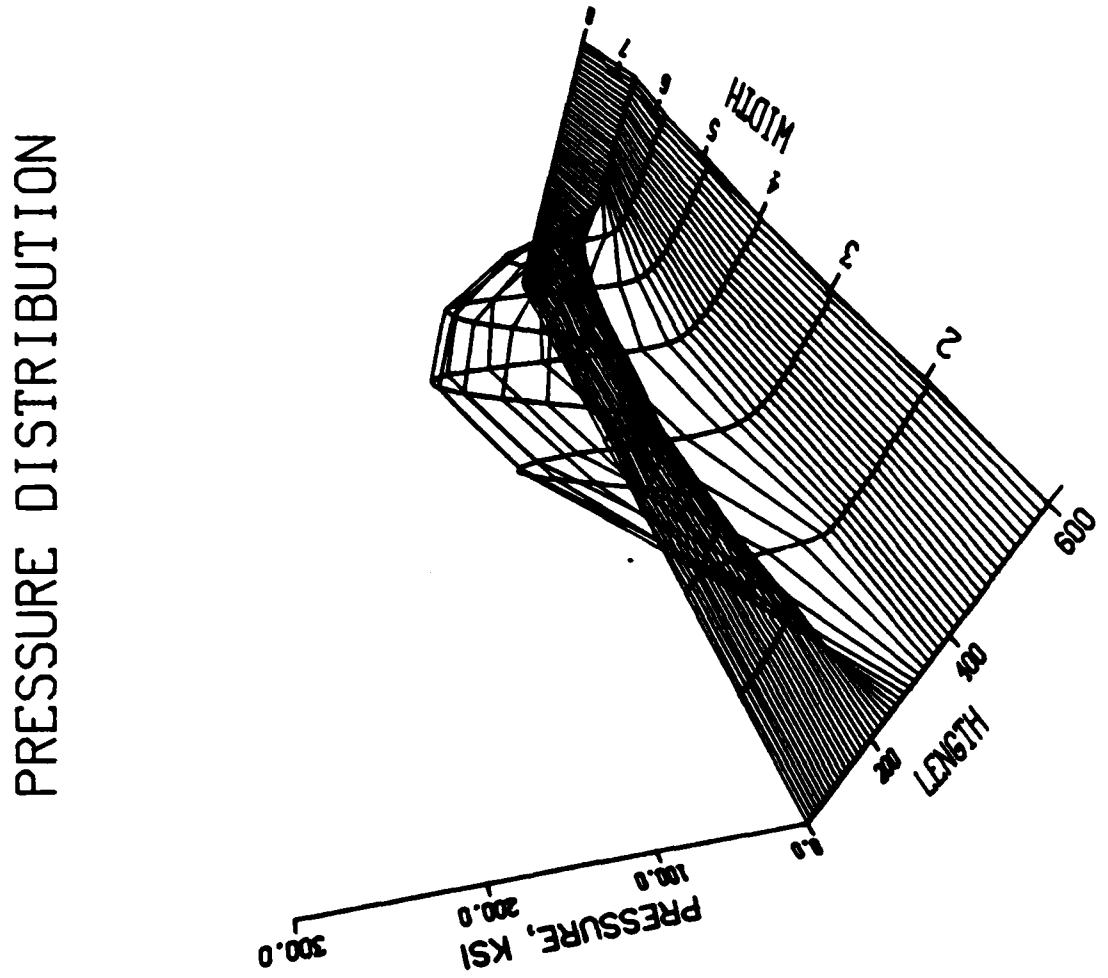

Figure 17A. Surface pressure and temperature distribution for Santotrac 50 at 29C and 2.0 percent slip.

TEMPERATURE DISTRIBUTION

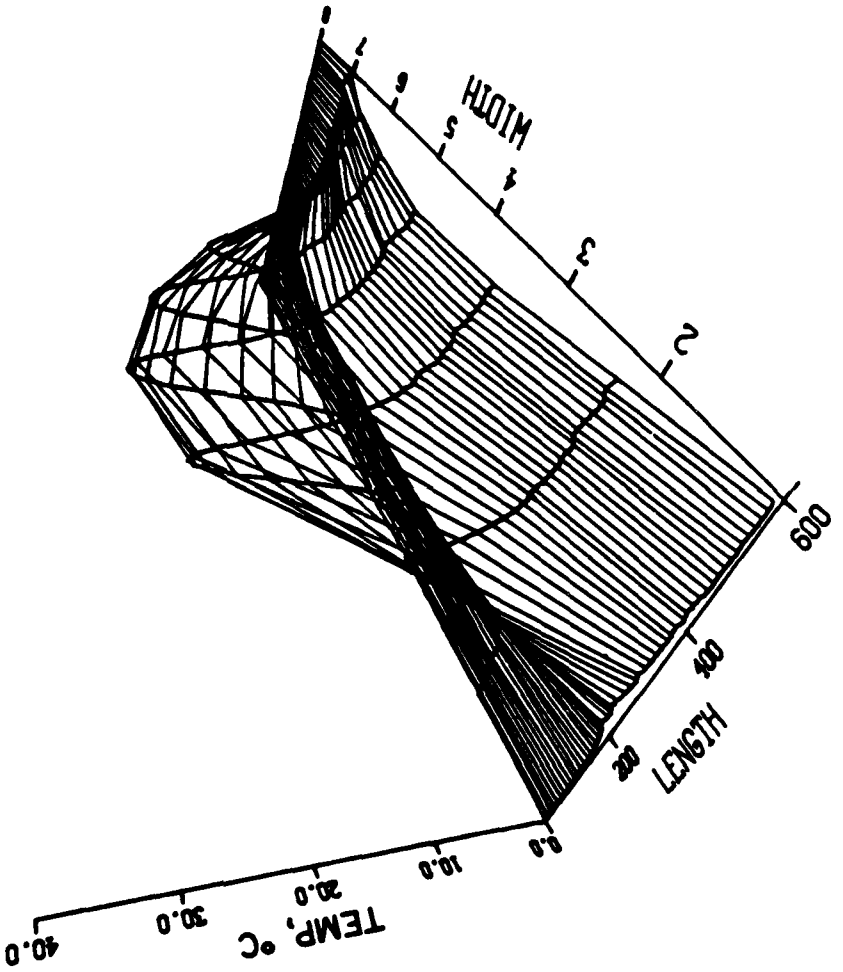

Figure 17B. Disk Load = 454 N (102 pounds)
Peak Pressure = 1.07 GPa (156 ksi)
Peak Temperature = 30C
Length Calibration = 3.12×10^{-3} mm/div (0.123 inch/div)
Width Calibration = 0.51 mm/div (0.020 inch/div)

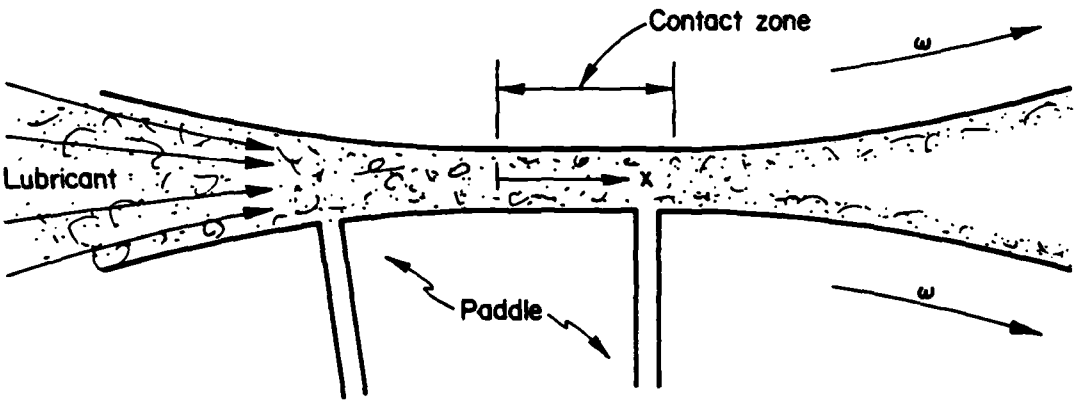

Figure 18. Traction transducer entering contact region of rolling disk.

Figure 19. Local traction transducer and mated test disk.

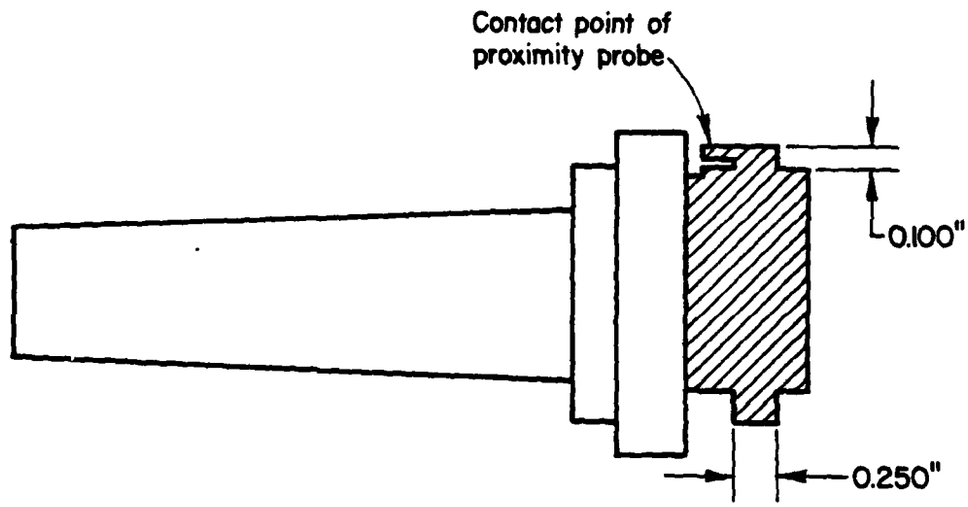

Figure 20. Cross section of disc showing details of traction measurement paddle.

(a) Averaged Waveform

$F_T(x)$

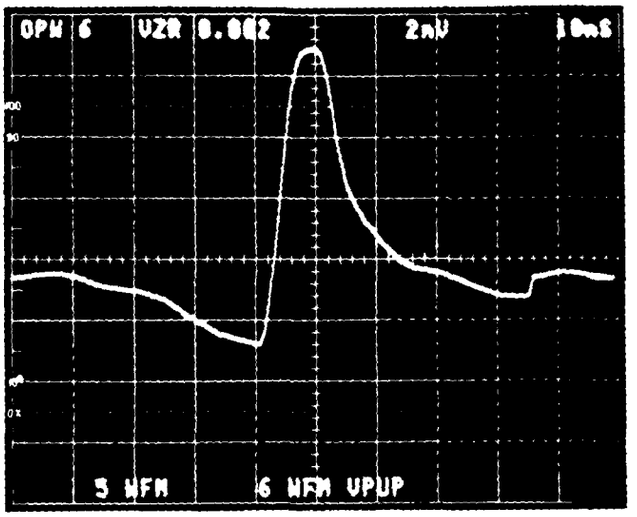

(b) Derivative of Waveform

$dF_T(x)/dx$

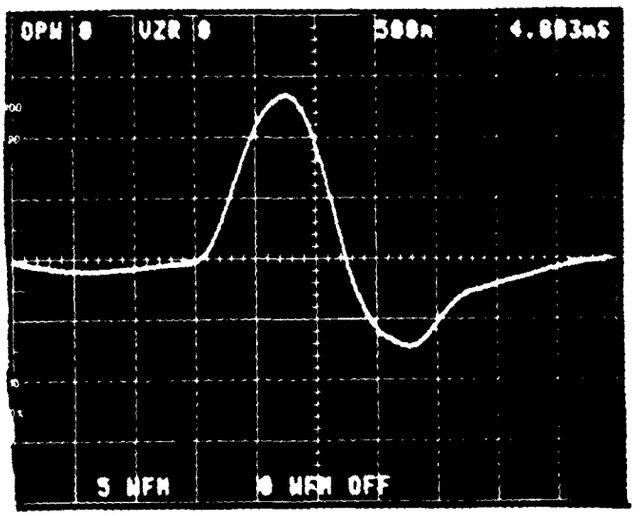

Figure 21. Traction transducer output.

Speed: 120 rpm 36.118 mm diameter disk (1.422 inches)
Load: 1.4 GPa (200 ksi)
Traction: 31 N (7 pounds)
Scope Sweep: 10ms/div (upper trace)
4.803ms/div (lower trace)

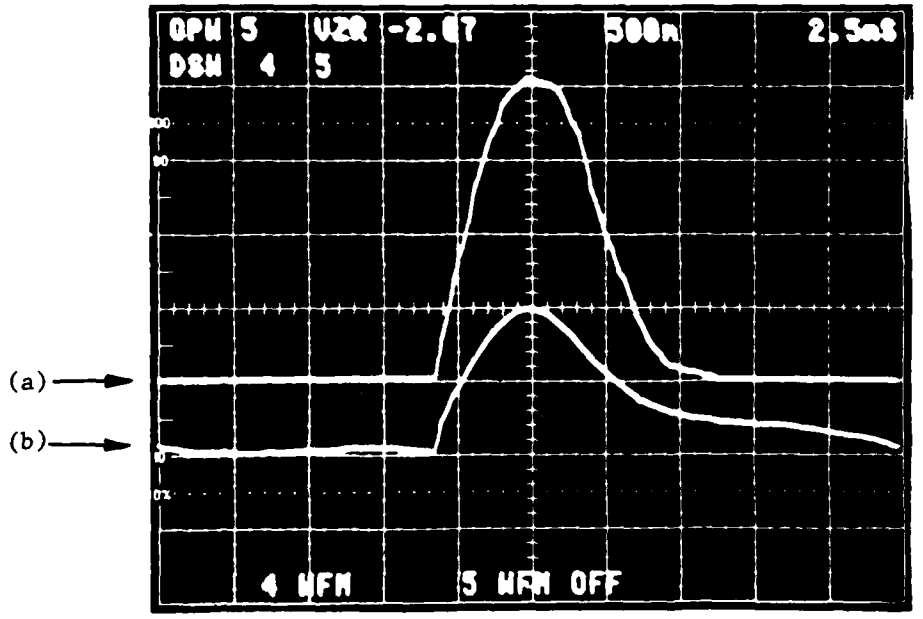

(a) inlet contact region

(b) outlet contact region

Figure 22. Differentiated traction transducer output.

Speed: 120 rpm 36.118 mm diameter disk (1.422 inches)
Load: 1.4 GPa (200 ksi)
Traction: 31 N (7 pounds)
Scope Sweep: 2.5ms/div

REFERENCES

1. Kannel, J. W. and Dow, T. A., "The Relation Between Pressure and Temperature in a Rolling/Sliding EHD Contact". Trans. ASLE, Vol. 23, No. 3, p 262 (July 1980).

2. Dow, T. A., "A Heat Balance in an EHD Contact", presented at the ASME Winter Annual Meeting, November 1980. (See also ONR Technical Report dated May 22, 1980).

3. Alsaad, M., Bair, S., Sanborn, D. M. and Winer, W. O., "Glass Transi-Tion in Lubricants: Its Relation to Elastohydrodynamic Lubrication", (EHD) School of Mechanical Engineering, Georgia Insitute of Technology report, April 1977.

4. Johnson, K. L., and Teuaarwerk, "Shear Behavior of Elastohydrodynamic Oil Films", Proc. R. Society London A, 356, 1977, pp 215-236.

5. Miller, R. S., "On the Mechanical Behavior of Entrance Materials in Concentrated Contacts", Trans. ASLE, Vol. 19, pp 1-16.

6. Montrose, C. J., Moynihan, C. T. and Sasabe, J., "Dynamic Shear and Structural Viscoelasticity in Elastohydrodynamic Lubrication", Catholic University report to ONR.

7. Bell, J. C., Kannel, J. W., and Allen, C. M., "The Rheological Behavior of a Lubricant in the Contact Zone of a Rolling-Contact System", Trans. ASME J. of Basic Eng., Vol. 68, Series D, No. 3, Sept. 1964, pp 423-435.

8. Kannel, J. W., and Walowit, J. A., "Simplified Analysis for Tractions Between Rolling-Sliding Elastohydrodynamic Contacts", ASME Trans., Vol. 93, Series F, No. 1, January 1971, pp 39-44.


DATE
FILME
8